Monoclonal Invariant NKT (iNKT) Cell Mice Reveal a Role for Both Tissue of Origin and the TCR in Development of iNKT Functional Subsets

Eleanor Clancy-Thompson, Gui Zhen Chen, Paul M. Tyler, Mariah M. Servos, Marta Barisa, Patrick J. Brennan, Hidde L. Ploegh and Stephanie K. Dougan

Supplementary Material	http://www.jimmunol.org/content/suppl/2017/05/31/jimmunol.1700214.DCSupplemental
References	This article **cites 58 articles**, 28 of which you can access for free at: http://www.jimmunol.org/content/199/1/159.full#ref-list-1

Why *The JI*? Submit online.

- **Rapid Reviews! 30 days*** from submission to initial decision

- **No Triage!** Every submission reviewed by practicing scientists

- **Fast Publication!** 4 weeks from acceptance to publication

*average

Subscription	Information about subscribing to *The Journal of Immunology* is online at: http://jimmunol.org/subscription
Permissions	Submit copyright permission requests at: http://www.aai.org/About/Publications/JI/copyright.html
Email Alerts	Receive free email-alerts when new articles cite this article. Sign up at: http://jimmunol.org/alerts

Monoclonal Invariant NKT (iNKT) Cell Mice Reveal a Role for Both Tissue of Origin and the TCR in Development of iNKT Functional Subsets

Eleanor Clancy-Thompson,* Gui Zhen Chen,* Paul M. Tyler,* Mariah M. Servos,* Marta Barisa,† Patrick J. Brennan,‡ Hidde L. Ploegh,†,1 and Stephanie K. Dougan*,†,1

Invariant NKT (iNKT) cell functional subsets are defined by key transcription factors and output of cytokines, such as IL-4, IFN-γ, IL-17, and IL-10. To examine how TCR specificity determines iNKT function, we used somatic cell nuclear transfer to generate three lines of mice cloned from iNKT nuclei. Each line uses the invariant Vα14Jα18 TCRα paired with unique Vβ7 or Vβ8.2 subunits. We examined tissue homing, expression of PLZF, T-bet, and RORγt, and cytokine profiles and found that, although monoclonal iNKT cells differentiated into all functional subsets, the NKT17 lineage was reduced or expanded depending on the TCR expressed. We examined iNKT thymic development in limited-dilution bone marrow chimeras and show that higher TCR avidity correlates with higher PLZF and reduced T-bet expression. iNKT functional subsets showed distinct tissue distribution patterns. Although each individual monoclonal TCR showed an inherent subset distribution preference that was evident across all tissues examined, the iNKT cytokine profile differed more by tissue of origin than by TCR specificity. *The Journal of Immunology*, 2017, 199: 159–171.

NKT cells are a subset of T cells that primarily recognize lipid Ags in a complex with the class I MHC homolog CD1d (1, 2). Type II NKT cells carry a diverse TCR repertoire, recognize a variety of lipid Ags, such as sulfatides, and will not be discussed further in this article. In mice, type I NKT cells (invariant NKT [iNKT]) express an invariant Vα14Jα18 TCRα-chain, paired with a limited, but diverse, set of TCRβ-chains. Vβ8.1, 8.2, 7, 8.3, and 2 are preferentially used, but the CDR3 regions vary widely, such that iNKT cells form a polyclonal pool (3). iNKT cells are activated by the ligand α-galactosylceramide (α-GalCer) (1, 4). Other known Ags include self- and microbial lipids (5). Under conditions of infection or inflammation, iNKT cells can skew the ensuing immune response by rapidly producing cytokines, such as IFN-γ, IL-13, and IL-4, without an obligate need for proliferation (1).

Functional subsets of iNKT cells exist, and they are classified according to the expression of signature transcription factors during thymic development or by the production of signature cytokines. T-bet, PLZF, and RORγt delineate NKT1, NKT2, and NKT17 subsets in the thymus; they produce IFN-γ, IL-4, or IL-17, respectively (6–8). The three major iNKT cell subsets likely differentiate during thymic development, as most convincingly shown by single-cell transcriptional profiling of thymic NKT1, NKT2, NKT17, and NKT0 cells (9). Whether interconversions among iNKT subsets can occur is not known. Production of NKT17 cells appears to be driven by particular signaling pathways; ThPOK and PTEN expression inversely correlate with acquisition of a RORγt⁺ IL-17–producing phenotype (10, 11), whereas mTORC2 is required for NKT17 development (12). Oxidized 5 methylcytosine in DNA suppresses NKT17 development, as revealed by an overabundance of hyperactivated NKT17 cells in mice lacking the epigenetic regulators Tet2 and Tet3 (13). Other subsets of iNKT cells, including IL-10–producing NKT10 cells (14), follicular helper-like iNKT cells (15), IL-9–producing iNKT cells (16), and regulatory iNKT cells (11, 17) have been described, but there is no evidence for thymic instruction of these subsets. Certain iNKT subsets are enriched in particular tissues; adipose tissue contains PLZF⁻E4BP4⁺ IL-10–producing iNKT cells with a regulatory phenotype (18, 19), whereas skin-draining lymph nodes are enriched in NK1.1⁻CD4⁻CD44⁺ NKT17 cells (20, 21). NKT2 cells are more frequently found in mesenteric lymph nodes, at least in BALB/c mice (7). In a model of tuberculosis infection, iNKT cells producing GM-CSF were crucial for control of infection in the lung (22). Liver-resident and spleen-resident iNKT cells differ in their ability to reject B16 melanoma lung metastases (23).

Recognition of α-GalCer occurs predominantly through the TCRα-chain, with the TCRβ-chain forming contacts only with CD1d (24). Nevertheless, Vβ-chain usage may influence the

spectrum of ligands recognized by iNKT cells (25). Cocrystal structures of TCR, ligand, and CD1d, together with careful measurements of binding kinetics, suggest that ligand merely determines the off-rate of TCR binding (26–29). Indeed, in contrast to most class I MHC–restricted TCRs, the iNKT TCR adopts a similar docking mode independent of the identity of the ligand bound (30–33). In contrast, a library of recombinant iNKT TCRs with different TCRβ-chains showed differential recognition of molecules such as iGb3, GSL-1, and other ligands thought to be more physiologically relevant than α-GalCer (34). Similar effects of TCRβ mutations on ligand recognition were observed for human iNKT TCRs (35), and indeed, selective loss of high-affinity iNKT cells has been observed in several human diseases (36, 37). Retrogenic mice expressing several discrete, natural, or engineered iNKT TCRs showed that positive selection of iNKT cells correlated with TCR affinity, whereas lineage choice between NKT1 versus NKT2 was more strongly correlated with the half-life of TCR association (38). iNKT cell TCR fine specificity may play a role in recognition of self-lipids, because Vβ7$^+$ iNKT cells have a higher affinity for self-lipids and are preferentially selected in the thymus (39) despite having a lower affinity for α-GalCer than Vβ8$^+$ iNKT cells (40).

To examine the role of TCR specificity in iNKT cell effector differentiation, we performed somatic cell nuclear transfer (SCNT) using the nuclei of individual iNKT cells to generate three independent lines of transnuclear (TN) mice, all of which use the identical Vα14Jα18 TCRα-chain but with three distinct TCRβ rearrangements. We show by differential staining with OCH, α-GalCer, and α-glucosylceramide (α-Glc) tetramers that these iNKT cells recognize different ligands. No comparable set of mice producing distinct iNKT TCRs has been reported. Thus, these unique strains of mice allowed us to definitively address the contribution of TCR fine specificity to formation of functional iNKT cell subsets and their presence across different tissues. The Vβ7A and Vβ8.2 TCRs predisposed against NKT17 development across every tissue examined, whereas the Vβ7C TCR displayed increased NKT17 development. However, iNKT cells obtained from different tissues showed strikingly disparate functions, irrespective of TCR usage. Therefore, TCR specificity plays a minor role in iNKT cell lineage choice.

Materials and Methods

Animal care

Animals were housed at the Whitehead Institute for Biomedical Research and at the Dana-Farber Cancer Institute and were maintained according to the National Institutes of Health (NIH) *Guide for the Care and Use of Laboratory Animals* and protocols approved by the MIT Committee on Animal Care and the Dana-Farber Cancer Institute Institutional animal Care and Use Committee, respectively. C57BL/6, BALB/c, and RAG2$^{-/-}$ mice were purchased from The Jackson Laboratory. Jα18$^{-/-}$ mice were obtained from Dr. M. Brenner (Boston, MA).

TN mouse generation

TN mice were generated as previously described (41–43). Briefly, CD1d-PBS57 tetramer$^+$Vβ7$^+$ cells were sorted by FACS and used as a source of donor nuclei for SCNT. The mitotic spindle was removed from mouse oocytes and replaced with donor nuclei. The nucleus-transplanted oocytes were then activated in medium containing strontium and Trichostatin A and allowed to develop in culture to the blastocyst stage. SCNT blastocysts were used to derive embryonic stem cell lines. These embryonic stem cell lines were then injected into wild-type B6×DBA F1 blastocysts and implanted into pseudopregnant females. The resulting chimeric pups were mated to C57BL/6 females to establish the Vβ7A and Vβ7C lines. Vβ8.2 mice were generated by intercrossing the Vβ7C and TRP1^{high} mouse lines (42) and selecting for founder progeny that received a single copy of the Vα14Jα18 TCR rearrangement and a single copy of the Vβ8.2 TCR rearrangement. Mice were backcrossed for seven generations to C57BL/6

mice (nine generations for RAG2$^{-/-}$ crossed lines). F1 mice were generated by crossing seven-generation C57BL/6-backcrossed males to BALB/c females. Vα14 mice used throughout the study were littermates of the Vβ7A, Vβ7C, or Vβ8.2 mice used. Mice were used at 6–12 wk of age, and both males and females were included. For each experiment, five mice were included per group. A mix of ages and both sexes were included per group, with age and sex matching among the groups as closely as possible. No correlation was observed between age and any of the parameters examined or sex and any of the parameters examined.

Sequencing of the TCR genes

iNKT cells were sorted by FACS for CD1d-PBS57 tetramer$^+$ cells and used as a source of RNA. 5′RACE was performed according to the manufacturer's protocol (Number L1502-01, GeneRacer; Invitrogen). Gene sequences were searched against the IEDB database (http://www.iedb.org).

Tissue preparation

Lymphocytes were harvested from spleen, thymus, and lymph nodes by crushing organs through a 40-μm cell strainer. Adipose tissue was minced with a scalpel and digested in 5 mg/ml collagenase II for 30 min at 37°C with rotation. Lung tissue was placed in gentleMACS C Tubes (130-093-237) and digested using Lung Dissociation Kit enzymes (130-095-927) and the gentleMACS Dissociator (130-093-235; all from Miltenyi Biotec), as per the manufacturer's recommendation. Liver was homogenized through a 70-μm cell strainer and centrifuged at 1400 rpm for 5 min. The organ pellet was resuspended in 10 ml of 35% Percoll (17-0891-01; GE Healthcare) in RPMI 1640. A bottom layer of 70% Percoll in PBS was added before centrifugation at 1700 rpm for 15 min with no brakes. The middle layer of lymphocytes was harvested into 10 ml of PBS.

Flow cytometry

Cells were harvested from spleen, thymus, lymph nodes, liver, epididymal fat pads, or lung. Cell preparations were subjected to hypotonic lysis to remove erythrocytes, stained, and analyzed using a BD LSRFortessa. CD1d-PBS57 (CD1d-αgal) tetramers were obtained from the NIH Tetramer Core Facility. CD1d α-GlcCer, α-GalCer (24:1), and OCH tetramers were generated as previously reported with minor modifications (44). Briefly, α-Glc (phytosphingosine base, C26:0 N-acyl chain), α-GalCer (C24:1 N-acyl chain), or OCH (both lipids kindly provided by Gurdyal Besra) were solubilized in PBS with 0.25% sodium taurocholate (Sigma) and then incubated at a 5:1 molar ratio with mouse CD1d (NIH Tetramer Core Facility) for 16 h at 37°C before tetramer assembly with fluorophore-lined streptavidin (Life Technologies). The following Abs were from BioLegend: IFN-γ (clone XMG1.2, catalog number [cat. no.] 505830), IL-4 (clone 11B11, cat. no. 504109), IL-17A (clone TC11-18H10.1, cat. no. 506916), Tbet (clone 4B10, cat. no. 644816), Vβ7 (clone TR310, cat. no. 118306), CD3 (clone 17A2, cat. no. 100236), CD3ε (clone 145-2C11, cat. no. 100330), and CD4 (clone RM4-5, cat. no. 100531). The following Abs were from eBioscience: RORγt (clone B2D, cat. no. 17-6981-80) and PLZF (clone Mags.21F7, cat. no. 53-9320-82).

Cell culturing

Cells were cultured in RPMI 1640 medium supplemented with 10% heat-inactivated FBS, 2 mM L-glutamine, 100 U/ml penicillin G sodium, 100 μg/ml streptomycin sulfate, 1 mM sodium pyruvate, 0.1 mM nonessential amino acids, and 0.1 mM 2-ME. For stimulation cultures, total cell preparations from the indicated organs were stimulated with PMA and ionomycin for 4 h in the presence of GolgiStop (Invitrogen). Cells were then fixed, permeabilized, and stained with Abs to IL-4, IFN-γ, and IL-17. Alternatively, total lymph node cells were stimulated with 100 ng/ml α-GalCer (Avanti Polar Lipids), and production of IFN-γ in 24-h culture supernatants was measured by ELISA, as indicated (BD Pharmingen).

Results

Generation of iNKT TN mice

SCNT is a unique tool used to clone mice from Ag-specific lymphocytes (41–43, 45, 46), including from iNKT cell nuclei (47). A previous report of TN iNKT cell mice only used mice that express the Vα14-rearranged TCR and relied on polyclonal Vβ expression (47). This yields a mouse model similar to the Vα14 TCR-transgenic line (4). To address the contribution of Vβ usage to iNKT cell subset specification, we generated three distinct mouse lines, cloned from the nuclei of individual

iNKT cells (Fig. 1A). The subset identity of the original nuclei donors was not determined; however, all epigenetic marks are erased by nuclear reprogramming, such that only the DNA-encoded TCR rearrangements are retained in the germline-transmitting TN mouse lines. All three lines use the canonical Vα14Jα18 TCRα rearrangement; two lines express Vβ7 rear-

rangements with unique CDR3 sequences (A and C), and the remaining line uses Vβ8.2 (Table I). When the Vβ8.2 line was further crossed to a CD1d$^{-/-}$ background, iNKT cells failed to develop, consistent with wild-type iNKT cells (data not shown). Because the TCRα and TCRβ loci map to different chromosomes, backcrossing to C57BL/6 mice yielded mice that retained only the
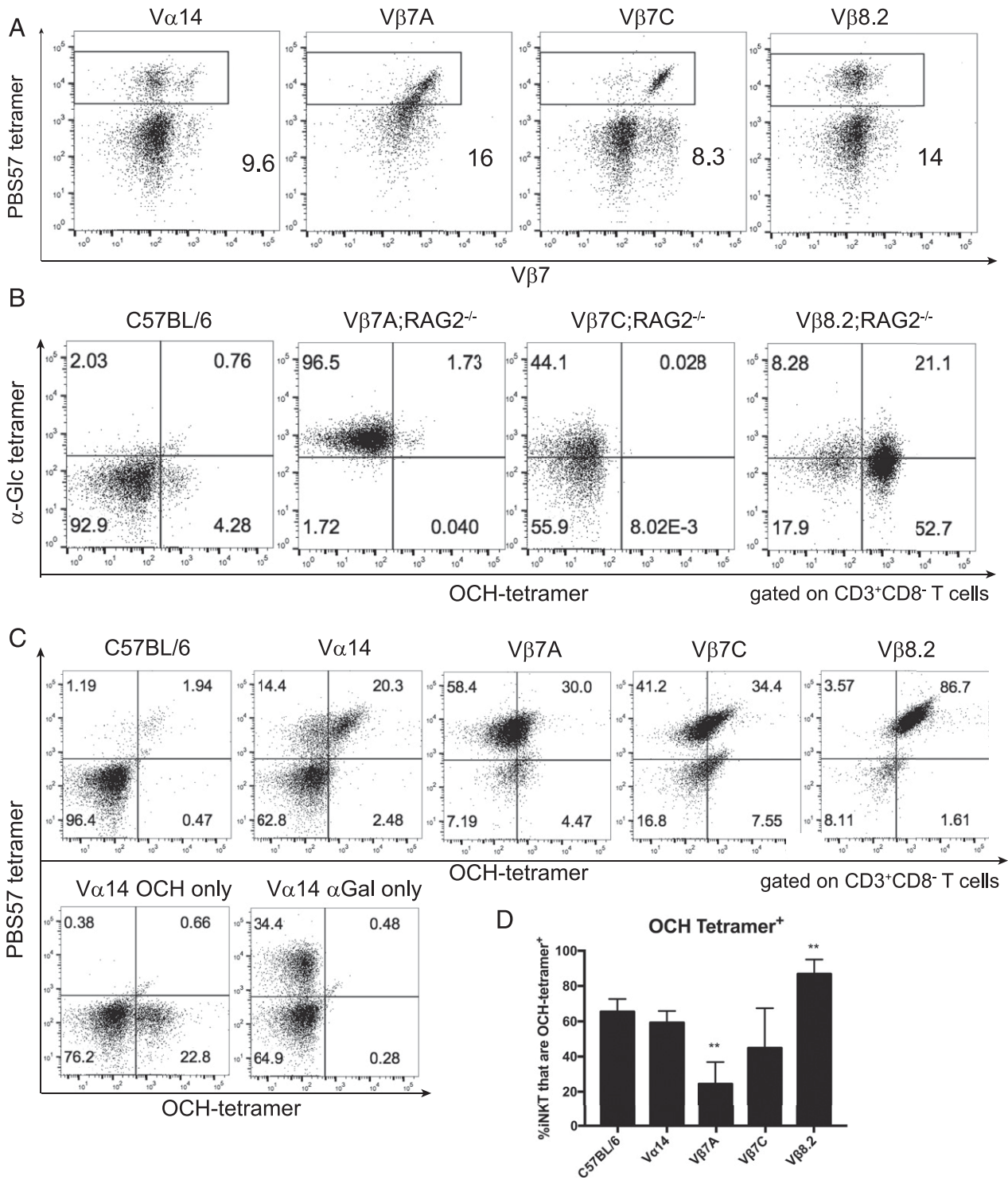
FIGURE 1. iNKT TN mice have monoclonal iNKT cells with distinct antigenic specificities. (**A**) Splenocytes were isolated from the indicated TN mouse lines and stained with anti-Vβ7, CD1d (PBS57) tetramer, and anti-CD4. Results are representative of >50 mice per group. (**B**) Splenocytes were isolated from the indicated C57BL/6 or TN mouse lines and stained with anti-CD3, anti-CD8, OCH tetramer, and α-Glc tetramer. Both tetramers were added simultaneously. Plots are gated on CD3$^+$CD8$^-$ T cells. (**C**) Thymocytes from C57BL/6 or TN mouse lines were isolated and stained with anti-CD3 and OCH tetramer. Cells were washed before being stained with CD1d (PBS57) tetramers to assess displacement. (**D**) Quantification of OCH staining across multiple independent experiments. **$p < 0.01$ versus C57BL/6.

Table I.   TCR sequences from iNKT TN mouse lines

	Variable	CDR3	Joining
Vβ7A	TRBV29	CASSPPGQGGRVFF	Trbj 1–7
Vβ7C	TRBV29	CASSLPGHNERLFF	Trbj 2–4
Vβ8.2	TRBV13-3	CASSDRGYEQYF	Trbj 2–7

```
                 FR1-IMGT            CDR1-IMGT        FR2-IMGT
                  (1-26)             (27-38)          (39-55)

           1      10       20        30        40         50
Vβ7A   DMKVTQMPRYLIKRMGENVLLECGQD MSH.......ET MYWYRQDPGLGLQLIYI
Vβ7C   DMKVTQMPRYLIKRMGENVLLECGQD MSH.......ET MYWYRQDPGLGLQLIYI
Vβ8.2  EAAVTQSPRSKVAVTGGKVTLSCHQT NNH.......DY MYWYRQDTGHGLRLIHY


       CDR2-IMGT               FR3-IMGT                    CDR3            D-J
        (56-65)                (66-104)

          60       70       80        90        100
       SYD....VDS NSEGDIP.KGYRVSRK.KREHFSLILDSAKTNQTSVYFC ASSPPGQGGRVFFGKGTRLTVV
       SYD....VDS NSEGDIP.KGYRVSRK.KREHFSLILDSAKTNQTSVYFC ASSLPGHNERLFFGHGTKLSVL
       SYV....ADS TEKGDIP.DGYKASRP.SQENFSLILELASLSQTAVYFC ASSDRGYEQYFGPGTRLTVL
```

TCRα TN locus (Vα14 line). These mice have an increased frequency of polyclonal iNKT cells that use the same restricted Vβ pattern seen in C57BL/6 mice.

Monoclonal iNKT cells have different ligand specificities

The three iNKT TCRs differ in their ligand specificities. Although all three bind α-GalCer tetramers, Vβ7A iNKT cells stain exclusively with α-Glc tetramers, Vβ7C iNKT cells stain dimly with α-Glc tetramers, and Vβ8.2 iNKT cells stain brightly with OCH tetramers, when the two tetramers are added simultaneously in a competitive binding assay (Fig. 1B). Single staining with α-Glc and OCH tetramers revealed that, even without competition, Vβ7A and Vβ7C iNKT cells stain dimly with OCH, whereas Vβ8.2 iNKT cells (like C57BL/6 mice) can bind α-Glc and OCH tetramers equally well (Supplemental Fig. 1A). OCH tetramers also stained Vβ8.2 cells, even in the presence of equimolar α-GalCer–CD1d (PBS57) tetramers (Supplemental Fig. 1B). In addition, each of the monoclonal lines was stained first with excess OCH tetramer, washed, and then stained with CD1d (PBS57) tetramer; we find very little OCH staining of Vβ7A and Vβ7C iNKT cells compared with Vβ8.2 iNKT cells (Fig. 1C). Compared over multiple experiments, Vβ8.2 iNKT cells are consistently more positive for OCH compared with the other monoclonal iNKT cells (Fig. 1D). As would be expected from monoclonal lines, the staining patterns of OCH tetramer binding were similar, regardless of whether cells were isolated from thymus, spleen, or skin-draining lymph node, although the intensity of tetramer staining varied by organ (Supplemental Fig. 1B). Competition between OCH and a version of α-GalCer with a naturally occurring lipid tail length (24.1) shows exclusive staining with α-GalCer 24.1 for Vβ7A and Vβ7C iNKT cells, whereas Vβ8.2 and Vα14 iNKT cells stain α-GalCer 24.1 and OCH (Supplemental Fig. 1C). Altogether, these results confirm differential ligand recognition among our three monoclonal iNKT TN mouse lines, and they are similar to those found by Cameron et al. (34).

TN iNKT cells are similar to C57BL/6 iNKT cells but with increased abundance

We examined expression of CD4, CD44, and NK1.1, which are commonly used to distinguish subpopulations of iNKT cells. CD44 and NK1.1 expression patterns were similar to polyclonal

iNKT cells and varied more by tissue of origin than by TCR (Supplemental Fig. 2A, 2B). Monoclonal iNKT cells expressed CD4 at similar frequencies to iNKT cells from C57BL/6 mice (Supplemental Fig. 2C).

Although C57BL/6 mice have few iNKT cells in most organs except liver, Vα14 TN mice have abundant iNKT cells in all tissues examined, including lung and adipose tissue, making them a useful source of polyclonal iNKT cells (Fig. 2A). We next examined iNKT cell tissue distribution in each of the iNKT TN mouse lines. Numbers of iNKT cells were determined for each organ analyzed and added to estimate the total number of iNKT cells per mouse. From each of the monoclonal mouse lines (Vβ7A, Vβ7C, and Vβ8.2), we recovered 29–35 million iNKT cells per animal compared with 25 million for the Vα14 line and <4 million for C57BL/6 mice (Fig. 2B). Compared with C57BL/6 mice, all iNKT TN lines have increased numbers of iNKT cells in lymph nodes, as expected, given that iNKT cells represent the majority of T cells in these lines. None of the monoclonal iNKT lines showed obvious differences in relative tissue distribution of iNKT cells compared with the polyclonal iNKT cells in Vα14 mice (Fig. 2B). When stimulated in vitro with PMA and ionomycin, TN Vα14 iNKT cells produced IL-17, IFN-γ, and IL-4 at similar levels and frequencies as those seen from B6 iNKT cells (Fig. 2C).

iNKT cells contribute to pathology in several autoimmune diseases, yet all iNKT TN lines are fertile, remain healthy, and showed no evidence of morbidity up to 1 y of age. The TN mice used were hemizygous for the TN TCR genes to allow for development of conventional CD4$^+$ and CD8$^+$ T cells (Fig. 3A), as well as Foxp3$^+$ regulatory T cells (Tregs) (Fig. 3B). Thymic development was mostly normal in TN mice, albeit with reduced populations of CD4$^+$CD8$^+$ cells, indicating a more rapid transit of T cells with rearranged TCRα- and TCRβ-chains (Fig. 3A, 3C), as also seen for conventional TCR-transgenic mice and mice expressing a Vα14Jα18-transgenic TCRα (4). To determine whether potentially autoreactive iNKT cells were constrained by Foxp3$^+$ Tregs, we crossed each iNKT TN line to RAG2$^{-/-}$ mice. All iNKT TN;RAG2$^{-/-}$ mice are similarly viable and remain healthy with normal lifespans, despite having exclusively CD1d tetramer$^+$ T cells that were not obviously anergic, as evidenced by
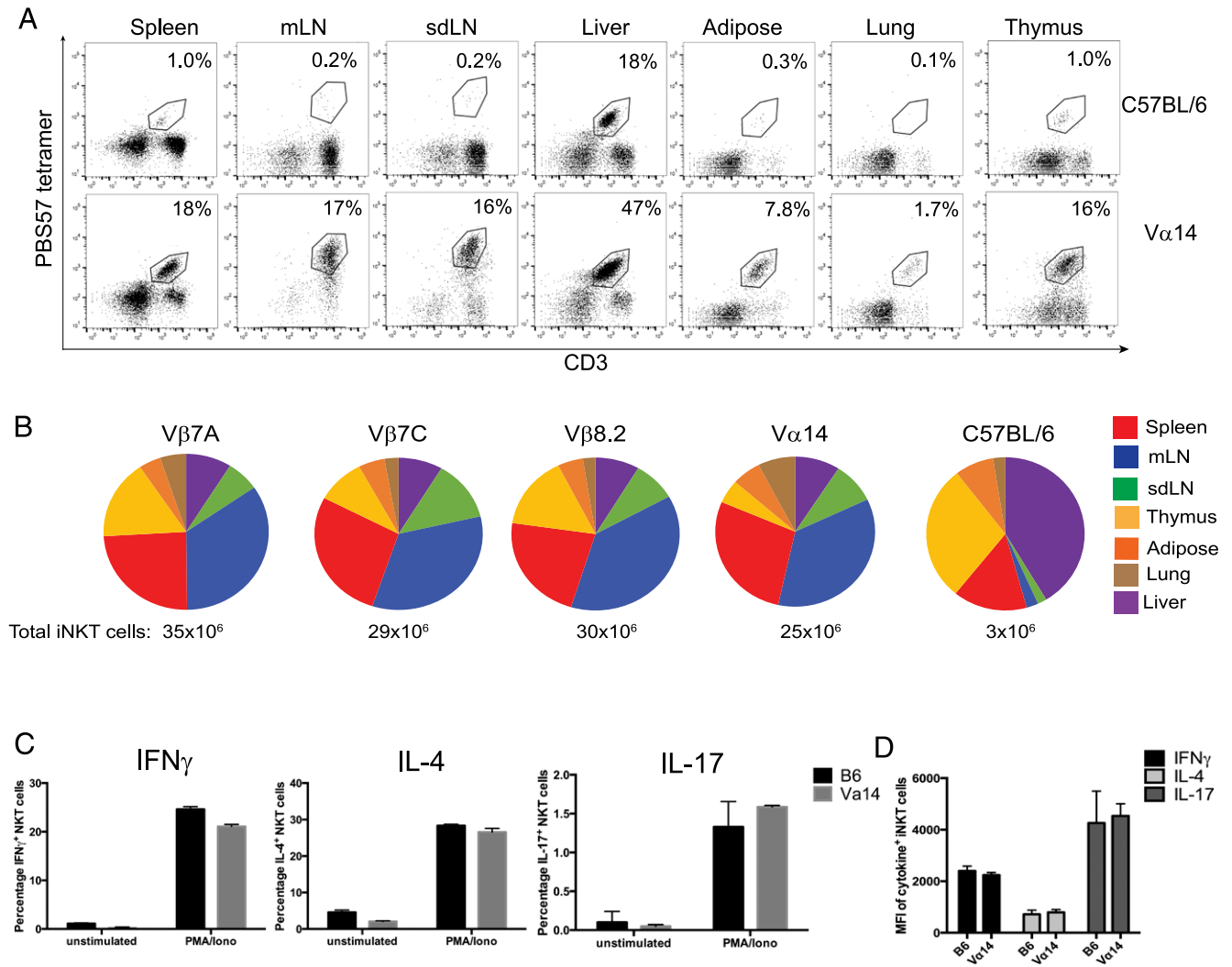
FIGURE 2. iNKT TN mice have increased frequencies of iNKT cells. (**A**) iNKT cells were harvested from the spleen, mesenteric lymph nodes (mLN), skin-draining lymph nodes (sdLN), liver, adipose tissue, lungs, and thymus of C57BL/6 and Vα14 mice and stained with anti-CD3 and CD1d (PBS57) tetramer. Results are representative of five mice per group; averaged in (**B**). (B) Lymphocytes were harvested from the spleen, mesenteric lymph nodes (mLN), skin-draining lymph nodes (sdLN), liver, adipose tissue, lungs, and thymus of the indicated mice and counted. Cells were stained with anti-CD3 and CD1d (PBS57) tetramer and analyzed by flow cytometry. The percentage of iNKT cells from each organ was multiplied by the cell count and added to obtain an estimated frequency of total iNKT cells in the body. Results shown are the average of five to eight mice per group. (**C**) Splenocytes from C57BL/6 and Vα14 mice were stimulated in vitro with PMA/ionomycin for 4 h in the presence of GolgiStop. Cells were stained with anti-CD3 and CD1d (PBS57) tetramer before they were fixed, permeabilized, and stained with anti–IFN-γ, anti–IL-4, and anti–IL-17. Results shown are gated on CD3$^+$CD1d-tetramer$^+$ cells. Results shown are representative of three independent experiments with $n = 3$ biological replicates. (**D**) Quantification of the MFI of cytokine-positive iNKT cells.

their capacity to produce IFN-γ upon stimulation with α-GalCer (Fig. 3D–F). These data suggest that factors other than the presence of iNKT cells are required for pathologies in which iNKT cells have been implicated.

NKT1, NKT2, and NKT17 functional subsets are detectable in all monoclonal TN lines

To address the role of TCR fine specificity in iNKT subset specification, we stimulated iNKT cells from Vα14, Vβ7A, Vβ7C, and Vβ8.2 mice with PMA/ionomycin and measured production of signature cytokines by intracellular staining. NKT1, NKT2, and NKT17 cells were clearly detectable in all monoclonal mouse lines (Supplemental Fig. 3); however, the frequency of NKT17 cells in Vβ7A and Vβ8.2 mice trended toward lower abundance (Supplemental Fig. 3A). NKT1 cells are the predominant subset in C57BL/6 mice and in our iNKT TN lines, which are on a

C57BL/6 background. To determine whether TCR specificity might influence iNKT subset differentiation in backgrounds other than C57BL/6, we generated F1 crosses of each iNKT TN line to BALB/c. The resulting F1 mice showed a higher frequency of NKT2 cells, as expected. Vα14 thymi had higher frequencies of IL-4–producing cells than did any of the monoclonal lines, although this difference disappeared in the periphery (Fig. 4). Again, all three functional subsets were present in monoclonal Vβ7A, Vβ7C, and Vβ8.2 mice, with Vβ7A and Vβ8.2 TCRs skewing slightly away from the NKT17 lineage (Fig. 4). These results also argue against potential artifacts induced by insufficient backcrossing of the original founding TN chimeras to C57BL/6.

NKT17 cells are a small population, representing only 1–3% of total iNKT cells in C57BL/6 or BALB/c mice. The greatest populations of IL-17–producing iNKT cells are found in the
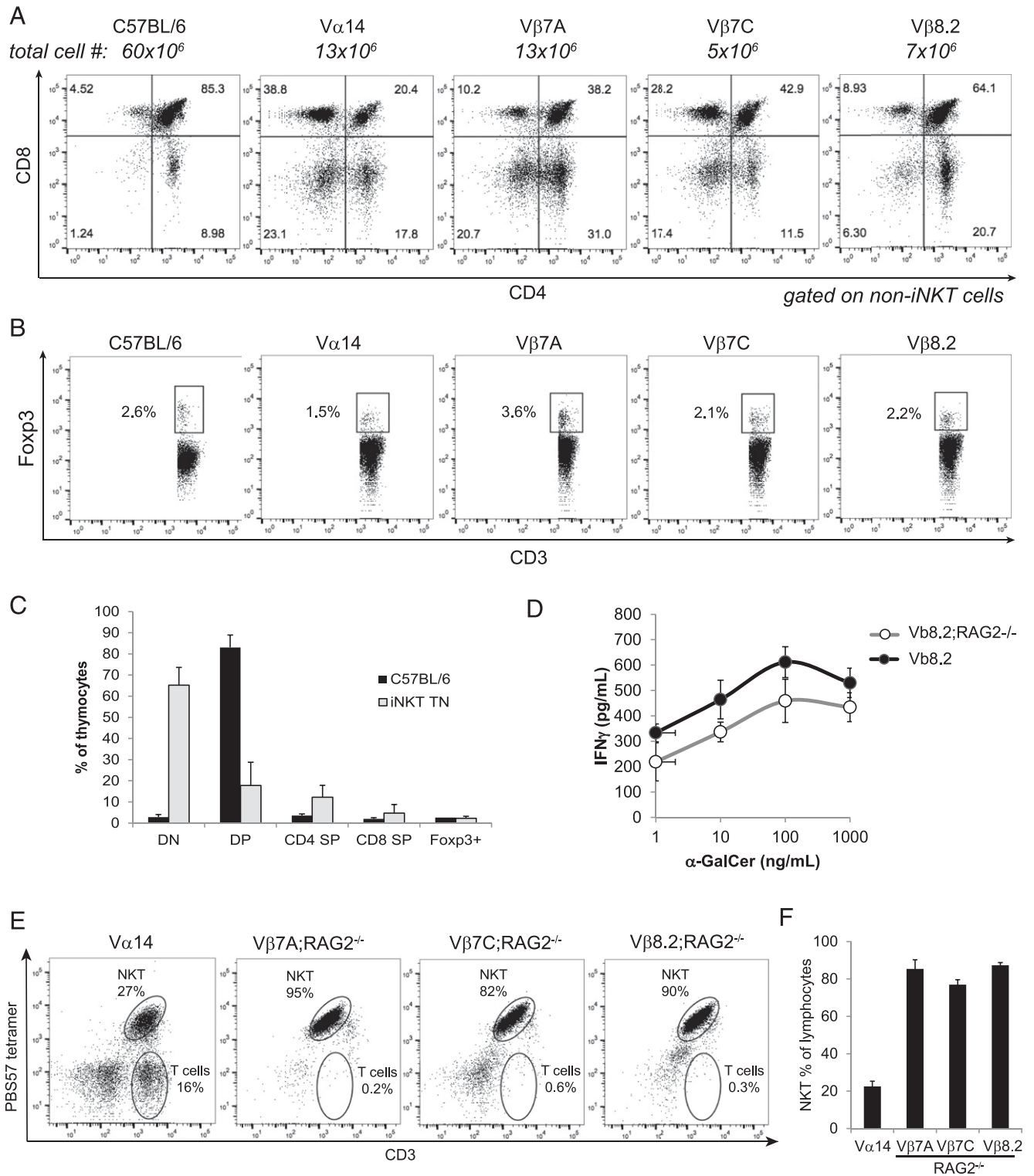
FIGURE 3. Conventional CD4, CD8, and Foxp3$^+$ Tregs develop in hemizygous RAG-proficient iNKT TN mice. (**A**) Thymocytes from C57BL/6 and all TN lines were stained with anti-CD3, CD1d (PBS57) tetramer, anti-CD4, and anti-CD8. Results shown are gated on non-iNKT cells (CD3$^+$CD1d-tetramer$^-$). (**B**) Thymocytes from C57BL/6 and all TN lines were stained with anti-CD3 and CD1d (PBS57) tetramer before being fixed, permeabilized, and stained with anti-Foxp3. Results shown are gated on non-iNKT cells. (**C**) Quantification of (A) and (B), $n = 3$ mice per group. (**D**) Lymph node cells from Vβ8.2 and Vβ8.2; RAG2$^{-/-}$ mice were stimulated with the indicated concentrations of α-GalCer. IFN-γ was measured in 24-h culture supernatants by ELISA. Error bars are SD. (**E**) Each monoclonal TN line was crossed to RAG2$^{-/-}$ background. Peripheral blood of mice of the indicated genotypes was stained with CD1d (PBS57) tetramer and anti-CD3. (**F**) Quantification of (E) averaged over five mice per group.

skin-draining lymph nodes, as previously reported (21). To better visualize NKT17 cells, we examined skin-draining lymph node cells from each monoclonal TN line on RAG-sufficient and RAG-deficient backgrounds. Vβ7A and Vβ8.2 mice had fewer NKT17 cells, whereas the Vβ7C TCR favored NKT17 development (Fig. 5). These trends were evident, even when the TN genes were crossed onto a RAG-deficient background to prevent further V(D)J rearrangements (Fig. 5).
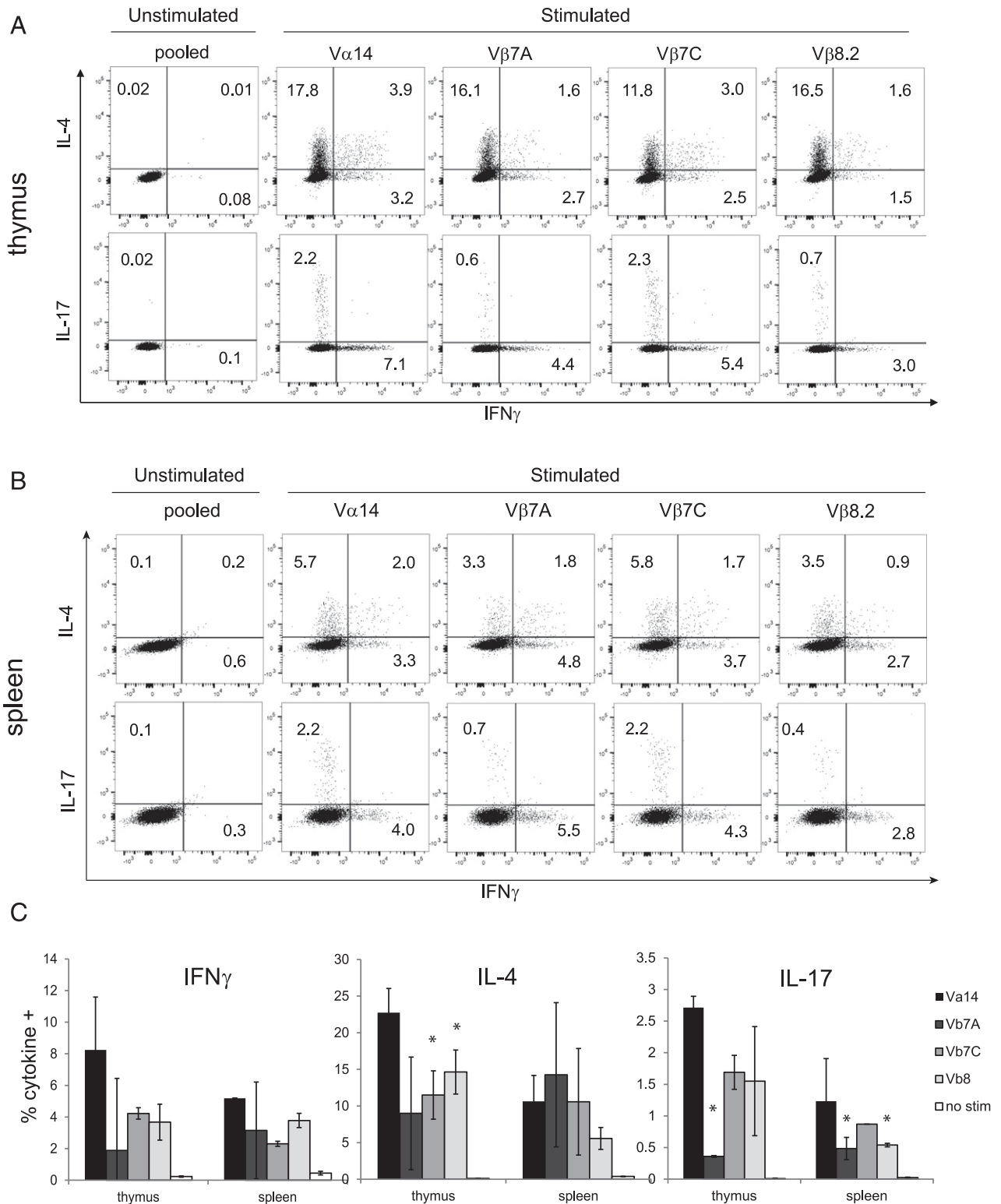
FIGURE 4. Monoclonal iNKT cells can produce all major cytokines. Cells from thymus (**A**) or spleen (**B**) of B6×Balb/c F1 mice of all TN lines were stimulated in vitro with PMA/ionomycin for 4 h in the presence of GolgiStop. Cells were stained with anti-CD3 and CD1d (PBS57) tetramer before being fixed, permeabilized, and stained with Abs to IFN-γ, IL-4, and IL-17. Results shown are gated on CD3⁺CD1d-tetramer⁺ cells. (**C**) Quantification of (A) and (B). *$p < 0.05$ versus Vα14. $n = 4$ mice per group. Error bars are SD.

Lineage development in the thymus correlates with iNKT TCR avidity

iNKT cells are selected in the thymus on CD1d-expressing double-positive thymocytes (48). As a surrogate for TCR signaling, we examined Nur77 expression in the thymus of Vα14 TN mice. Similarly to wild-type iNKT cells (49), Vα14 iNKT cells that are stage 0 (CD44^{lo}NK1.1⁻CD24⁺ iNKT cells) showed increased levels of TCR stimulation in the thymus, by Nur77 positivity (data not shown). We did not see significant levels of Nur77 in any peripheral tissues; however, iNKT cells in peripheral tissues could be induced to express Nur77 upon i.v. delivery of α-GalCer (data not shown).
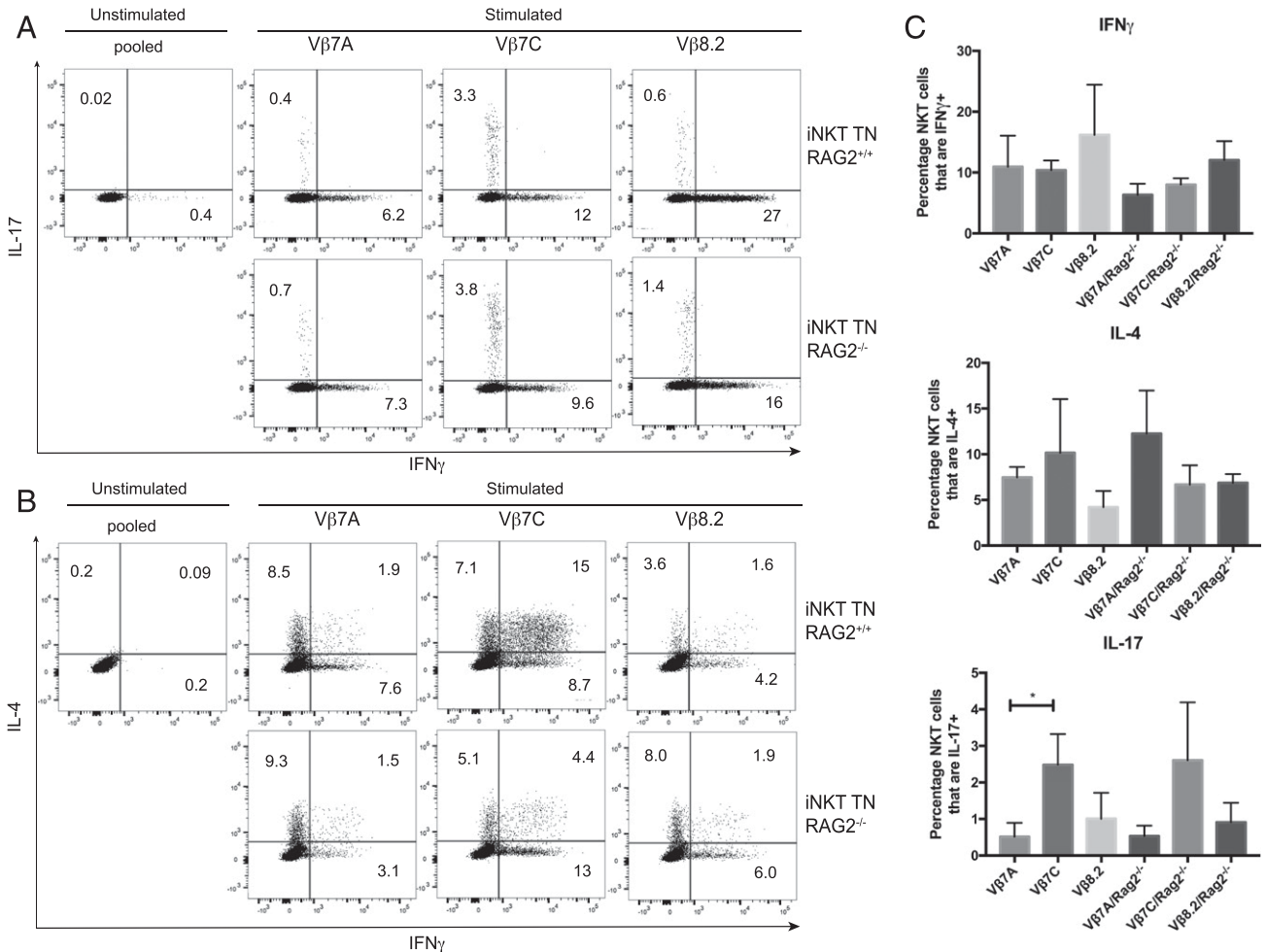
FIGURE 5.   NKT1, NKT2, and NKT17 subsets are present in rigorously monoclonal mice. (**A** and **B**) Skin-draining lymph node cells from all TN mice were stimulated in vitro with PMA/ionomycin for 4 h in the presence of GolgiStop. Cells were stained with anti-CD3 and CD1d (PBS57) tetramer, before being fixed, permeabilized, and stained with Abs to IFN-γ, IL-4, and IL-17. Results shown are gated on CD3$^+$CD1d-tetramer$^+$ cells. TN mice are either RAG proficient (upper panels) or RAG deficient (lower panels). (**C**) Quantification of (A) and (B), $n = 4$ mice per RAG2$^{+/+}$ group and $n = 3$ mice per RAG2$^{-/-}$ group. Mice were 5–6 wk of age, and both sexes were included in each group. $*p < 0.05$.

TN mice have greatly increased frequencies of iNKT cells in the thymus, demonstrating that positively selecting ligands are not limiting. However, increased numbers of iNKT cells may affect the development of iNKT cell functional subsets. Therefore, we generated mixed bone marrow chimeras consisting of 95% Jα18$^{-/-}$ bone marrow mixed with 5% iNKT TN bone marrow. In this setting, iNKT cells represent ∼1% of total thymocytes, similar to the level seen in C57BL/6 mice (Figs. 2A, 6A).

We examined thymic iNKT cells from the 95:5 bone marrow chimeric mice. Among the monoclonal TN lines, the iNKT TCR affinity for CD1d (PBS57) tetramer differs, with Vβ7A having the lowest affinity and Vβ8.2 having the highest affinity (Fig. 6A, 6C). However, tetramer$^+$ cells appear in a Gaussian distribution with respect to tetramer staining and CD3 expression (Fig. 6A). Because all of the iNKT cells in any given monoclonal line have identical affinities, differences in tetramer staining must be related to avidity. Indeed, the positive correlation between CD3 expression and tetramer staining suggests that surface TCR expression is a major contributor, although other factors that affect TCR avidity, such as expression of SLAM family members (50, 51), may be important. We looked at bright versus dim tetramer-stained cells with respect to their transcription factor profiles. Within each monoclonal line, we noticed that thymic iNKT cells with higher CD3 expression stained more brightly with tetramer and tended to

be PLZF^{bright} NKT2 cells, whereas lower avidity corresponded with T-bet$^+$ NKT1 development (Fig. 6B, 6D). These results are consistent with previous findings showing that Nur77 expression was positively correlated with IL-4 production in thymic iNKT cells (6) and with more recent findings showing that TCR half-life of binding to CD1d–lipid complexes correlates with NKT2 development (38).

Limited-dilution bone marrow chimeras reveal a role for the iNKT TCR in development of NKT17 cells

The 95:5 Jα18$^{-/-}$ to TN iNKT bone marrow chimera setting represents a more physiologic thymic development, and we examined whether monoclonal iNKT cells would display subset preferences in this setting. Cells were harvested from thymus, spleen, liver, and skin-draining lymph nodes and analyzed by intracellular cytokine staining (Fig. 7) and transcription factor staining (Fig. 8, Supplemental Fig. 4). We could detect NKT1, NKT2, and NKT17 cells in all organs and among all monoclonal lines using both methods. The subset distribution was dramatically different in different tissues, as reported previously (7, 19, 21). NKT1 cells were much more abundant in liver, whereas NKT17 cells were more abundant in skin-draining lymph nodes. However, within each organ, differences in cytokine production based on TCR were observed (Fig. 7, data not shown).
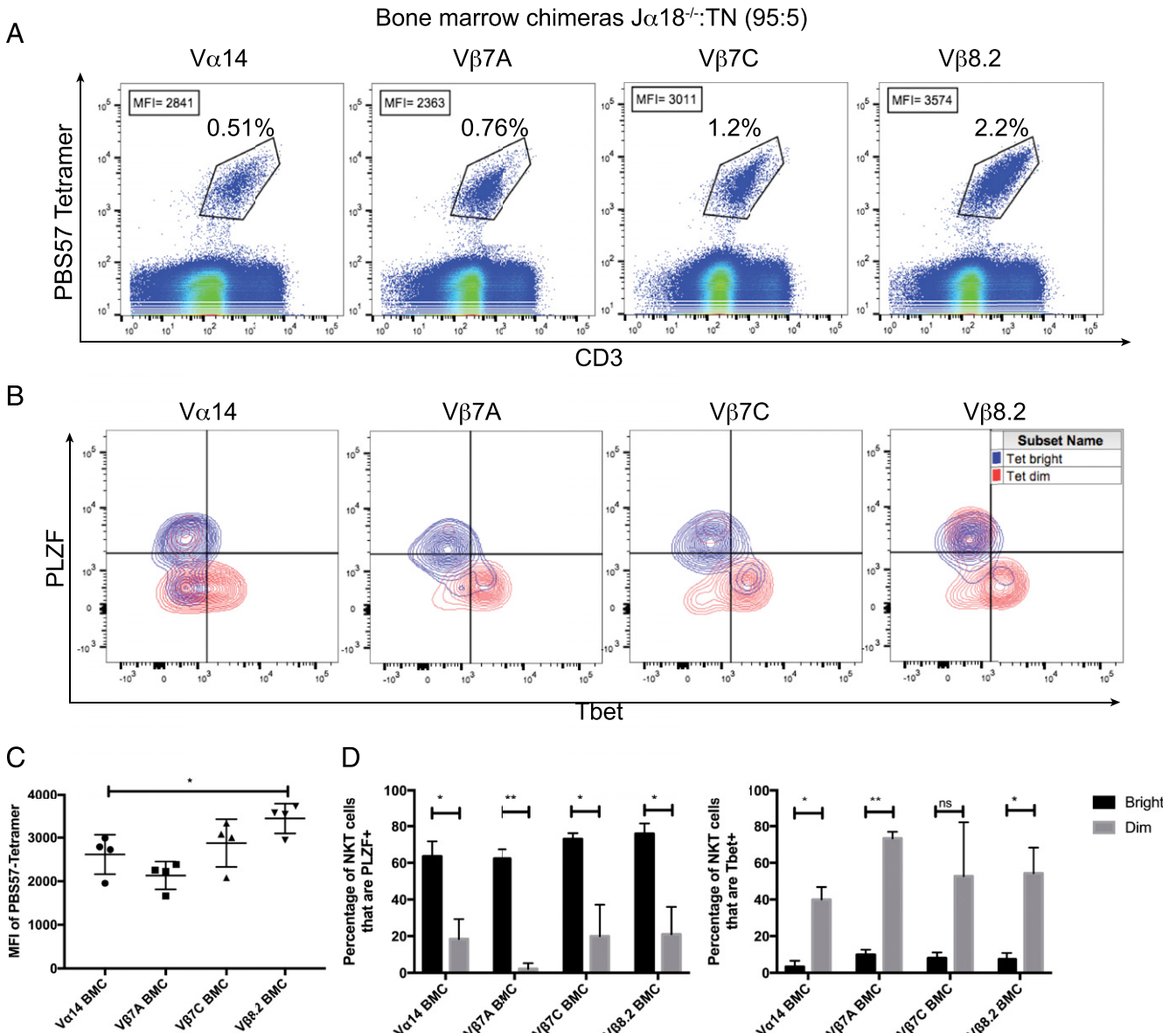
FIGURE 6. TCR avidity correlates with PLZF expression during thymic development of monoclonal iNKT cells. Jα18$^{-/-}$ mice were lethally irradiated, reconstituted with 95% Jα18$^{-/-}$ bone marrow and 5% bone marrow of the indicated TN lines, and analyzed 8 wk later. (**A**) Thymocytes from C57BL/6 mice and all TN lines were stained with anti-CD3 and CD1d (PBS57) tetramer and analyzed by flow cytometry. Mean fluorescence intensities (MFI) of tetramer staining for gated populations are shown within the plots. (**B**) Thymocytes from C57BL/6 mice and all TN lines were stained with anti-CD3 and CD1d (PBS57) tetramer before being fixed, permeabilized, and stained with Abs to PLZF, T-bet, and RORγt. Results shown are gated on CD1d (PBS57) tetramer$^+$ iNKT cells. Tet bright = top 20% of iNKT cells; Tet dim = bottom 20% of iNKT cells as defined by intensity of PE signal. (**C**) Quantification of mice shown in (A). *$p < 0.05$. (**D**) Quantification of mice shown in (B). $n = 4$ mice per group. *$p < 0.05$, **$p < 0.01$. Error bars are SD. ns, not significant.

To better profile the effect of a given TCR, independent of tissue of origin, we used intracellular cytokine data and normalized each data point to the average value for Vα14 polyclonal cells from the same organ (Fig. 7B). In this meta-analysis, Vβ7A iNKT cells showed significantly less IL-17 and less IL-4 production (Fig. 7), as well as reduced RORγt expression (Fig. 8), suggesting a decrease in NKT17 development in this monoclonal line. Vβ8.2 iNKT cells were also significantly less likely to become NKT17 cells (Figs. 7, 8) and trended toward increased IL-4 production and increased PLZF positivity (Figs. 7, 8), suggesting a propensity to become NKT2 cells. Vβ7C iNKT cells were significantly more likely to become NKT17 cells (Figs. 7, 8). All iNKT cells were similarly capable of IFN-γ production, demonstrating that the reduction in IL-17 production from Vβ7A and Vβ8.2 iNKT cells

is not because the cells are intrinsically refractory to stimulation but that they are skewed away from the NKT17 lineage.

Tissue of origin is a stronger predictor of iNKT function than TCR specificity

Although TCR specificity can influence NKT effector functions, particularly in settings of low precursor frequency (Fig. 6) (38), the largest determinant of iNKT effector function appeared to be tissue of origin. Indeed, when we categorized iNKT cells into NKT1, NKT2, and NKT17 based on their transcription factor profiles, we observed dramatically more NKT17 cells in skin-draining lymph nodes than in other tissues, regardless of TCR specificity (Fig. 8). Similarly, NKT1 cells were more prevalent in liver (Supplemental Fig. 4), and NKT2 cells were found more frequently in spleen and thymus (Supplemental Fig. 4). To determine the degree of influence

Bone marrow chimeras Jα18⁻/⁻:TN (95:5)
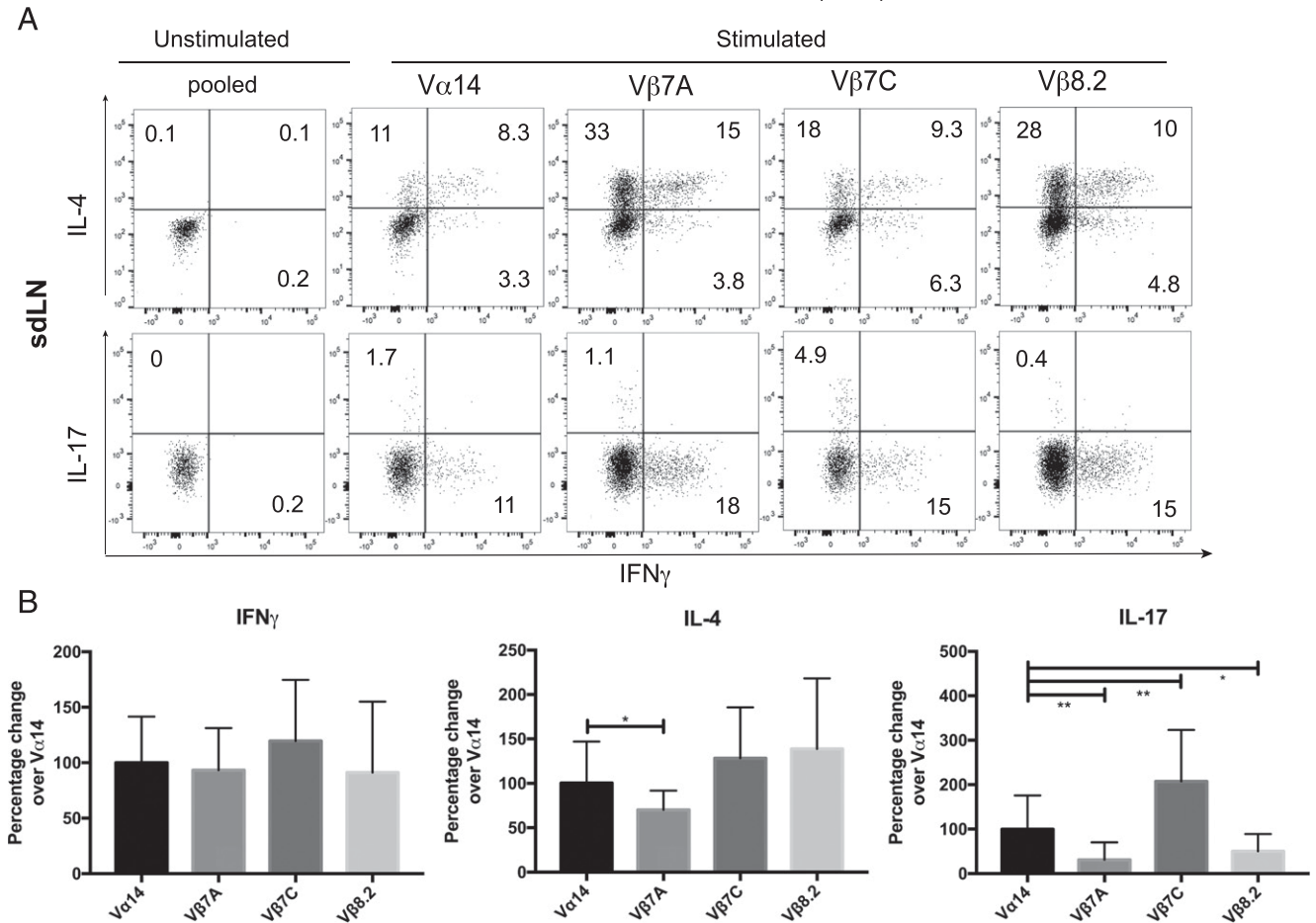
FIGURE 7. Limited-dilution bone marrow chimeras reveal a minor role for TCR specificity in lineage preference of iNKT cells. Jα18$^{-/-}$ mice were lethally irradiated, reconstituted with 95% Jα18$^{-/-}$ bone marrow and 5% bone marrow of the indicated TN lines, and analyzed 8 wk later. $n = 4$ mice per group. (**A**) Skin-draining lymph node (sdLN) cells from all TN mice were stimulated in vitro with PMA/ionomycin for 4 h in the presence of GolgiStop. Cells were stained with anti-CD3 and CD1d (PBS57) tetramer before being fixed, permeabilized, and stained with Abs to IFN-γ, IL-4, and IL-17. Results shown are gated on CD3^{+}CD1d-tetramer^{+} cells. (**B**) Quantification of intracellular cytokine staining data from thymus, spleen, skin-draining lymph nodes, and liver normalized to Vα14 values for the same organ. $*p < 0.05$, $**p < 0.01$. Error bars are SD.

of TCR specificity versus tissue of origin, we performed an ANOVA and revealed that, although TCR and tissue contribute to iNKT cell effector functions, tissue of origin accounts for a larger fraction of the observed variation (Fig. 8B).

Discussion

In this article, we unequivocally show that monoclonal iNKT cells with different ligand specificities differentiate in vivo into all iNKT subsets, albeit at altered frequencies. As is also the case for CD4^{+} Tregs (46, 52), in the setting of limited precursor frequency, iNKT cell lineage choice preferences become more apparent. CD1d-presented ligands are not limiting in the thymus, as shown in this article and by other investigators (38); however, particular ligands that might instruct development into NKT1, NKT2, or NKT17 lineages may be less abundant. Despite the subtle influence of TCR on NKT17 frequencies, tissue of origin had a more dominant role in predicting iNKT cell function, with iNKT cells from liver, skin-draining lymph nodes, and spleen having distinct cytokine and transcription factor profiles.

Whether iNKT lineage choice is determined in the thymus or the tissues is a subject of some debate. Several reports, including this one, have identified clear populations of NKT1, NKT2, and NKT17 cells in the thymus, which would suggest that lineage commitment

occurs in the thymus and that differential chemokine receptor expression explains the differences in accumulation of iNKT subsets in different tissues (7, 9, 53). A recent report by the Mallevaey group (38) correlated CD1d tetramer dissociation rates with NKT1 versus NKT2 thymic development, although no clear relationship between TCR binding kinetics and NKT17 development was determined. In the same study, cytokine production by acutely stimulated peripheral iNKT cells was similar across a range of TCR affinities and half-lives (38), suggesting that NKT subset imprinting in the thymus may be altered in the periphery as the result of differential accumulation of particular subsets or further differentiation upon arrival in tissues. The thymic imprinting model does not account for follicular helper iNKT cells, which arise postimmunization (15), IL-9–producing iNKT cells (16), or NKT10 cells, which may undergo further differentiation after seeding the adipose tissue (18, 19). Our observation that a given TCR influences subset choice suggests that iNKT subset formation may occur as early as the positive selection event in the thymus. However, because tissues also contain CD1d^{+} cells presenting a variety of lipid Ags, the TCR specificity may continue to have an instructive role in subset formation outside of the thymus as well.

Tissue-specific programming of immune cells has been described for macrophages and Foxp3^{+} Tregs. Macrophage subsets include alveolar macrophages in the lung, microglia in the brain,
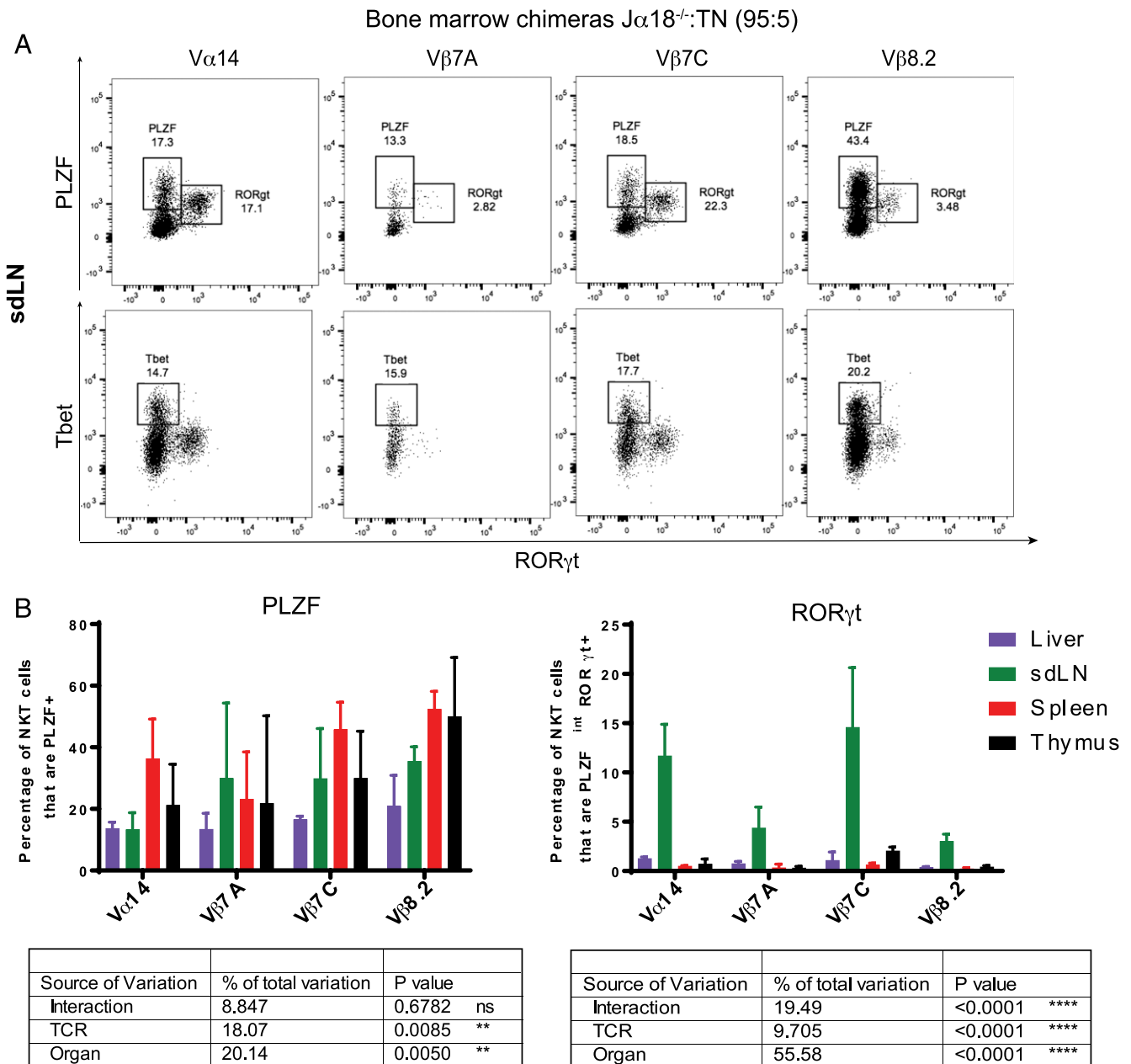
FIGURE 8. Tissue of origin plays a dominant role in cytokine profiles of monoclonal iNKT cells. $J\alpha 18^{-/-}$ mice were lethally irradiated, reconstituted with 95% $J\alpha 18^{-/-}$ bone marrow and 5% bone marrow of the indicated TN lines, and analyzed 8 wk later. $n = 4$ mice per group. (**A**) Skin-draining lymph node (sdLN) cells from all TN mice were stained with anti-CD3 and CD1d (PBS57) tetramer before being fixed, permeabilized, and stained with Abs to PLZF, T-bet, and RORγt. Results shown are gated on CD3$^+$CD1d-tetramer$^+$ cells. (**B**) Quantification of transcription factor expression as shown in (A). $n = 4$ mice per group. ANOVA was used to determine the relative contribution of TCR versus tissue of origin to explain the variation in transcription factor expression.

and Kupffer cells in the liver, all of which display unique transcriptional profiles. Macrophages are fairly plastic and can adapt to a new environment (54). Likewise, tissue-resident Tregs are present in adipose tissue, muscle, eye, and other sites, where they exert similar regulatory functions but express transcriptional profiles distinct from lymphoid-resident Tregs (55, 56). In an interesting analogy to iNKT cells, Tregs appear to seed tissues early in life (57). The factors that cause neonatal seeding of iNKT and Tregs into tissues remain to be identified. For iNKT cells, tissue-dependent reprogramming may occur, at least for adipose-resident iNKT cells that express a transcriptional profile distinct from their spleen or liver counterparts (18, 58).

In this article, we report four lines of TN mice with individual monoclonal populations of Vβ7 or Vβ8.2 iNKT cells. Although all three lines recognized α-GalCer, they showed differential recognition

of α-Glc and OCH, confirming different CD1d–lipid binding properties. These mice may be of great usefulness in addressing reactivity to particular gut microbial ligands or endogenous ligands. Furthermore, Vα14 TN mice are an excellent source of polyclonal iNKT cells, especially from tissues such as adipose or lung where infiltrating iNKT cells are in low abundance.

Acknowledgments

Disclosures

The authors have no financial conflicts of interest.

References

1. Bendelac, A., P. B. Savage, and L. Teyton. 2007. The biology of NKT cells. *Annu. Rev. Immunol.* 25: 297–336.

2. Macho-Fernandez, E., and M. Brigl. 2015. The extended family of CD1d-restricted NKT cells: sifting through a mixed bag of TCRs, antigens, and functions. *Front. Immunol.* 6: 362.

3. Guo, T., K. Chamoto, M. Nakatsugawa, T. Ochi, Y. Yamashita, M. Anczurowski, M. O. Butler, and N. Hirano. 2016. Mouse and human CD1d-self-lipid complexes are recognized differently by murine invariant natural killer T cell receptors. *PLoS One* 11: e0156114.

4. Bendelac, A., R. D. Hunziker, and O. Lantz. 1996. Increased interleukin 4 and immunoglobulin E production in transgenic mice overexpressing NK1 T cells. *J. Exp. Med.* 184: 1285–1293.

5. Birkholz, A. M., A. R. Howell, and M. Kronenberg. 2015. The alpha and omega of galactosylceramides in T cell immune function [Published erratum appears in 2015 *J. Biol. Chem.* 290: 20746]. *J. Biol. Chem.* 290: 15365–15370.

6. Lee, Y. J., K. L. Holzapfel, J. Zhu, S. C. Jameson, and K. A. Hogquist. 2013. Steady-state production of IL-4 modulates immunity in mouse strains and is determined by lineage diversity of iNKT cells. *Nat. Immunol.* 14: 1146–1154.

7. Lee, Y. J., H. Wang, G. J. Starrett, V. Phuong, S. C. Jameson, and K. A. Hogquist. 2015. Tissue-specific distribution of iNKT cells impacts their cytokine response. *Immunity* 43: 566–578.

8. Watarai, H., E. Sekine-Kondo, T. Shigeura, Y. Motomura, T. Yasuda, R. Satoh, H. Yoshida, M. Kubo, H. Kawamoto, H. Koseki, and M. Taniguchi. 2012. Development and function of invariant natural killer T cells producing T(h)2- and T(h)17-cytokines. *PLoS Biol.* 10: e1001255.

9. Engel, I., G. Seumois, L. Chavez, D. Samaniego-Castruita, B. White, A. Chawla, D. Mock, P. Vijayanand, and M. Kronenberg. 2016. Innate-like functions of natural killer T cell subsets result from highly divergent gene programs. *Nat. Immunol.* 17: 728–739.

10. Engel, I., M. Zhao, D. Kappes, I. Taniuchi, and M. Kronenberg. 2012. The transcription factor Th-POK negatively regulates Th17 differentiation in Vα14i NKT cells. *Blood* 120: 4524–4532.

11. Mattarollo, S. R., M. Yong, C. Gosmann, A. Choyce, D. Chan, G. R. Leggatt, and I. H. Frazer. 2011. NKT cells inhibit antigen-specific effector CD8 T cell induction to skin viral proteins. *J. Immunol.* 187: 1601–1608.

12. Wei, J., K. Yang, and H. Chi. 2014. Cutting edge: discrete functions of mTOR signaling in invariant NKT cell development and NKT17 fate decision. *J. Immunol.* 193: 4297–4301.

13. Tsagaratou, A., E. Gonzalez-Avalos, S. Rautio, J. P. Scott-Browne, S. Togher, W. A. Pastor, E. V. Rothenberg, L. Chavez, H. Lahdesmaki, and A. Rao. 2017. TET proteins regulate the lineage specification and TCR-mediated expansion of iNKT cells. *Nat. Immunol.* 18: 45–53.

14. Sag, D., P. Krause, C. C. Hedrick, M. Kronenberg, and G. Wingender. 2014. IL-10-producing NKT10 cells are a distinct regulatory invariant NKT cell subset. *J. Clin. Invest.* 124: 3725–3740.

15. King, I. L., A. Fortier, M. Tighe, J. Dibble, G. F. Watts, N. Veerapen, A. M. Haberman, G. S. Besra, M. Mohrs, M. B. Brenner, and E. A. Leadbetter. 2011. Invariant natural killer T cells direct B cell responses to cognate lipid antigen in an IL-21-dependent manner. *Nat. Immunol.* 13: 44–50.

16. Monteiro, M., A. Agua-Doce, C. F. Almeida, D. Fonseca-Pereira, H. Veiga-Fernandes, and L. Graca. 2015. IL-9 expression by invariant NKT cells is not imprinted during thymic development. *J. Immunol.* 195: 3463–3471.

17. Beaudoin, L., V. Laloux, J. Novak, B. Lucas, and A. Lehuen. 2002. NKT cells inhibit the onset of diabetes by impairing the development of pathogenic T cells specific for pancreatic beta cells. *Immunity* 17: 725–736.

18. Lynch, L., X. Michelet, S. Zhang, P. J. Brennan, A. Moseman, C. Lester, G. Besra, E. E. Vomhof-Dekrey, M. Tighe, H. F. Koay, et al. 2015. Regulatory iNKT cells lack expression of the transcription factor PLZF and control the homeostasis of T(reg) cells and macrophages in adipose tissue. *Nat. Immunol.* 16: 85–95.

19. Lynch, L., M. Nowak, B. Varghese, J. Clark, A. E. Hogan, V. Toxavidis, S. P. Balk, D. O'Shea, C. O'Farrelly, and M. A. Exley. 2012. Adipose tissue invariant NKT cells protect against diet-induced obesity and metabolic disorder through regulatory cytokine production. *Immunity* 37: 574–587.

20. Doisne, J. M., C. Becourt, L. Amniai, N. Duarte, J. B. Le Luduec, G. Eberl, and K. Benlagha. 2009. Skin and peripheral lymph node invariant NKT cells are mainly retinoic acid receptor-related orphan receptor (gamma)t+ and respond preferentially under inflammatory conditions. *J. Immunol.* 183: 2142–2149.

21. Michel, M. L., D. Mendes-da-Cruz, A. C. Keller, M. Lochner, E. Schneider, M. Dy, G. Eberl, and M. C. Leite-de-Moraes. 2008. Critical role of ROR-γt in a new thymic pathway leading to IL-17-producing invariant NKT cell differentiation. *Proc. Natl. Acad. Sci. USA* 105: 19845–19850.

22. Rothchild, A. C., P. Jayaraman, C. Nunes-Alves, and S. M. Behar. 2014. iNKT cell production of GM-CSF controls *Mycobacterium tuberculosis. PLoS Pathog.* 10: e1003805.

23. Crowe, N. Y., J. M. Coquet, S. P. Berzins, K. Kyparissoudis, R. Keating, D. G. Pellicci, Y. Hayakawa, D. I. Godfrey, and M. J. Smyth. 2005. Differential antitumor immunity mediated by NKT cell subsets in vivo. *J. Exp. Med.* 202: 1279–1288.

24. Borg, N. A., K. S. Wun, L. Kjer-Nielsen, M. C. Wilce, D. G. Pellicci, R. Koh, G. S. Besra, M. Bharadwaj, D. I. Godfrey, J. McCluskey, and J. Rossjohn. 2007. CD1d-lipid-antigen recognition by the semi-invariant NKT T-cell receptor. *Nature* 448: 44–49.

25. Pellicci, D. G., O. Patel, L. Kjer-Nielsen, S. S. Pang, L. C. Sullivan, K. Kyparissoudis, A. G. Brooks, H. H. Reid, S. Gras, I. S. Lucet, et al. 2009.

26. Wu, T. N., K. H. Lin, Y. J. Chang, J. R. Huang, J. Y. Cheng, A. L. Yu, and C. H. Wong. 2011. Avidity of CD1d-ligand-receptor ternary complex contributes to T-helper 1 (Th1) polarization and anticancer efficacy. *Proc. Natl. Acad. Sci. USA* 108: 17275–17280.

27. Patel, O., G. Cameron, D. G. Pellicci, Z. Liu, H. S. Byun, T. Beddoe, J. McCluskey, R. W. Franck, A. R. Castaño, Y. Harrak, et al. 2011. NKT TCR recognition of CD1d-α-C-galactosylceramide. *J. Immunol.* 187: 4705–4713.

28. Wun, K. S., G. Cameron, O. Patel, S. S. Pang, D. G. Pellicci, L. C. Sullivan, S. Keshipeddy, M. H. Young, A. P. Uldrich, M. S. Thakur, et al. 2011. A molecular basis for the exquisite CD1d-restricted antigen specificity and functional responses of natural killer T cells. *Immunity* 34: 327–339.

29. Mallevaey, T., A. J. Clarke, J. P. Scott-Browne, M. H. Young, L. C. Roisman, D. G. Pellicci, O. Patel, J. P. Vivian, J. L. Matsuda, J. McCluskey, et al. 2011. A molecular basis for NKT cell recognition of CD1d-self-antigen. *Immunity* 34: 315–326.

30. Li, Y., E. Girardi, J. Wang, E. D. Yu, G. F. Painter, M. Kronenberg, and D. M. Zajonc. 2010. The Vα14 invariant natural killer T cell TCR forces microbial glycolipids and CD1d into a conserved binding mode. *J. Exp. Med.* 207: 2383–2393.

31. Girardi, E., E. D. Yu, Y. Li, N. Tarumoto, B. Pei, J. Wang, P. Illarionov, Y. Kinjo, M. Kronenberg, and D. M. Zajonc. 2011. Unique interplay between sugar and lipid in determining the antigenic potency of bacterial antigens for NKT cells. *PLoS Biol.* 9: e1001189.

32. Pellicci, D. G., A. J. Clarke, O. Patel, T. Mallevaey, T. Beddoe, J. Le Nours, A. P. Uldrich, J. McCluskey, G. S. Besra, S. A. Porcelli, et al. 2011. Recognition of β-linked self glycolipids mediated by natural killer T cell antigen receptors. *Nat. Immunol.* 12: 827–833.

33. Yu, E. D., E. Girardi, J. Wang, and D. M. Zajonc. 2011. Cutting edge: structural basis for the recognition of β-linked glycolipid antigens by invariant NKT cells. *J. Immunol.* 187: 2079–2083.

34. Cameron, G., D. G. Pellicci, A. P. Uldrich, G. S. Besra, P. Illarionov, S. J. Williams, N. L. La Gruta, J. Rossjohn, and D. I. Godfrey. 2015. Antigen specificity of type I NKT cells is governed by TCR β-chain diversity. *J. Immunol.* 195: 4604–4614.

35. Chamoto, K., T. Guo, S. W. Scally, Y. Kagoya, M. Ancruzowski, C. H. Wang, M. A. Rahman, K. Saso, M. O. Butler, P. P. Chiu, et al. 2017. Key residues at third CDR3β position impact structure and antigen recognition of human invariant NK TCRs [Published erratum appears in 2017 *J. Immunol.* 198: 3757]. *J. Immunol.* 198: 1056–1065.

36. Tocheva, A. S., S. Mansour, T. G. Holt, S. Jones, A. Chancellor, J. P. Sanderson, E. Eren, T. J. Elliott, R. I. Holt, and S. D. Gadola. 2017. The clonal invariant NKT cell repertoire in people with type 1 diabetes is characterized by a loss of clones expressing high-affinity TCRs. *J. Immunol.* 198: 1452–1459.

37. Mansour, S., A. S. Tocheva, J. P. Sanderson, L. M. Goulston, H. Platten, L. Serhal, C. Parsons, M. H. Edwards, C. H. Woelk, P. T. Elkington, et al. 2015. Structural and functional changes of the invariant NKT clonal repertoire in early rheumatoid arthritis. *J. Immunol.* 195: 5582–5591.

38. Cruz Tleugabulova, M., N. K. Escalante, S. Deng, S. Fieve, J. Ereño-Orbea, P. B. Savage, J. P. Julien, and T. Mallevaey. 2016. Discrete TCR binding kinetics control invariant NKT cell selection and central priming. *J. Immunol.* 197: 3959–3969.

39. Wei, D. G., S. A. Curran, P. B. Savage, L. Teyton, and A. Bendelac. 2006. Mechanisms imposing the Vbeta bias of Valpha14 natural killer T cells and consequences for microbial glycolipid recognition. *J. Exp. Med.* 203: 1197–1207.

40. Schümann, J., M. P. Mycko, P. Dellabona, G. Casorati, and H. R. MacDonald. 2006. Cutting edge: influence of the TCR Vbeta domain on the selection of semi-invariant NKT cells by endogenous ligands. *J. Immunol.* 176: 2064–2068.

41. Dougan, S. K., J. Ashour, R. A. Karssemeijer, M. W. Popp, A. M. Avalos, M. Barisa, A. F. Altenburg, J. R. Ingram, J. J. Cragnolini, C. Guo, et al. 2013. Antigen-specific B-cell receptor sensitizes B cells to infection by influenza virus. *Nature* 503: 406–409.

42. Dougan, S. K., M. Dougan, J. Kim, J. A. Turner, S. Ogata, H. I. Cho, R. Jaenisch, E. Celis, and H. L. Ploegh. 2013. Transnuclear TRP1-specific CD8 T cells with high or low affinity TCRs show equivalent antitumor activity. *Cancer Immunol. Res.* 1: 99–111.

43. Dougan, S. K., S. Ogata, C. C. Hu, G. M. Grotenbreg, E. Guillen, R. Jaenisch, and H. L. Ploegh. 2012. IgG1+ ovalbumin-specific B-cell transnuclear mice show class switch recombination in rare allelically included B cells. *Proc. Natl. Acad. Sci. USA* 109: 13739–13744.

44. Brennan, P. J., R. V. Tatituri, M. Brigl, E. Y. Kim, A. Tuli, J. P. Sanderson, S. D. Gadola, F. F. Hsu, G. S. Besra, and M. B. Brenner. 2011. Invariant natural killer T cells recognize lipid self antigen induced by microbial danger signals. *Nat. Immunol.* 12: 1202–1211.

45. Kirak, O., E. M. Frickel, G. M. Grotenbreg, H. Suh, R. Jaenisch, and H. L. Ploegh. 2010. Transnuclear mice with predefined T cell receptor specificities against *Toxoplasma gondii* obtained via SCNT. *Science* 328: 243–248.

46. Bilate, A. M., D. Bousbaine, L. Mesin, M. Agudelo, J. Leube, A. Kratzert, S. K. Dougan, G. D. Victora, and H. L Ploegh. 2016. Tissue-specific emergence of regulatory and intraepithelial T cells from a clonal T cell precursor. *Sci. Immunol.* 1: eaaf7471.

47. Inoue, K., H. Wakao, N. Ogonuki, H. Miki, K. Seino, R. Nambu-Wakao, S. Noda, H. Miyoshi, H. Koseki, M. Taniguchi, and A. Ogura. 2005. Generation of cloned mice by direct nuclear transfer from natural killer T cells. *Curr. Biol.* 15: 1114–1118.

48. Pellicci, D. G., K. J. Hammond, A. P. Uldrich, A. G. Baxter, M. J. Smyth, and D. I. Godfrey. 2002. A natural killer T (NKT) cell developmental pathway involving a thymus-dependent NK1.1(−)CD4(+) CD1d-dependent precursor stage. *J. Exp. Med.* 195: 835–844.

49. Moran, A. E., K. L. Holzapfel, Y. Xing, N. R. Cunningham, J. S. Maltzman, J. Punt, and K. A. Hogquist. 2011. T cell receptor signal strength in Treg and iNKT cell development demonstrated by a novel fluorescent reporter mouse. *J. Exp. Med.* 208: 1279–1289.

50. Baev, D. V., S. Caielli, F. Ronchi, M. Coccia, F. Facciotti, K. E. Nichols, and M. Falcone. 2008. Impaired SLAM-SLAM homotypic interaction between invariant NKT cells and dendritic cells affects differentiation of IL-4/IL-10-secreting NKT2 cells in nonobese diabetic mice. *J. Immunol.* 181: 869–877.

51. Griewank, K., C. Borowski, S. Rietdijk, N. Wang, A. Julien, D. G. Wei, A. A. Mamchak, C. Terhorst, and A. Bendelac. 2007. Homotypic interactions mediated by Slamf1 and Slamf6 receptors control NKT cell lineage development. *Immunity* 27: 751–762.

52. Bautista, J. L., C. W. Lio, S. K. Lathrop, K. Forbush, Y. Liang, J. Luo, A. Y. Rudensky, and C. S. Hsieh. 2009. Intraclonal competition limits the fate determination of regulatory T cells in the thymus. *Nat. Immunol.* 10: 610–617.

53. Georgiev, H., I. Ravens, C. Benarafa, R. Förster, and G. Bernhardt. 2016. Distinct gene expression patterns correlate with developmental and functional traits of iNKT subsets. *Nat. Commun.* 7: 13116.

54. Lavin, Y., D. Winter, R. Blecher-Gonen, E. David, H. Keren-Shaul, M. Merad, S. Jung, and I. Amit. 2014. Tissue-resident macrophage enhancer landscapes are shaped by the local microenvironment. *Cell* 159: 1312–1326.

55. Burzyn, D., W. Kuswanto, D. Kolodin, J. L. Shadrach, M. Cerletti, Y. Jang, E. Sefik, T. G. Tan, A. J. Wagers, C. Benoist, and D. Mathis. 2013. A special population of regulatory T cells potentiates muscle repair. *Cell* 155: 1282–1295.

56. Cipolletta, D., M. Feuerer, A. Li, N. Kamei, J. Lee, S. E. Shoelson, C. Benoist, and D. Mathis. 2012. PPAR-γ is a major driver of the accumulation and phenotype of adipose tissue Treg cells. *Nature* 486: 549–553.

57. Olszak, T., D. An, S. Zeissig, M. P. Vera, J. Richter, A. Franke, J. N. Glickman, R. Siebert, R. M. Baron, D. L. Kasper, and R. S. Blumberg. 2012. Microbial exposure during early life has persistent effects on natural killer T cell function. *Science* 336: 489–493.

58. Cohen, N. R., P. J. Brennan, T. Shay, G. F. Watts, M. Brigl, J. Kang, and M. B. Brenner, ImmGen Project Consortium. 2013. Shared and distinct transcriptional programs underlie the hybrid nature of iNKT cells. *Nat. Immunol.* 14: 90–99.
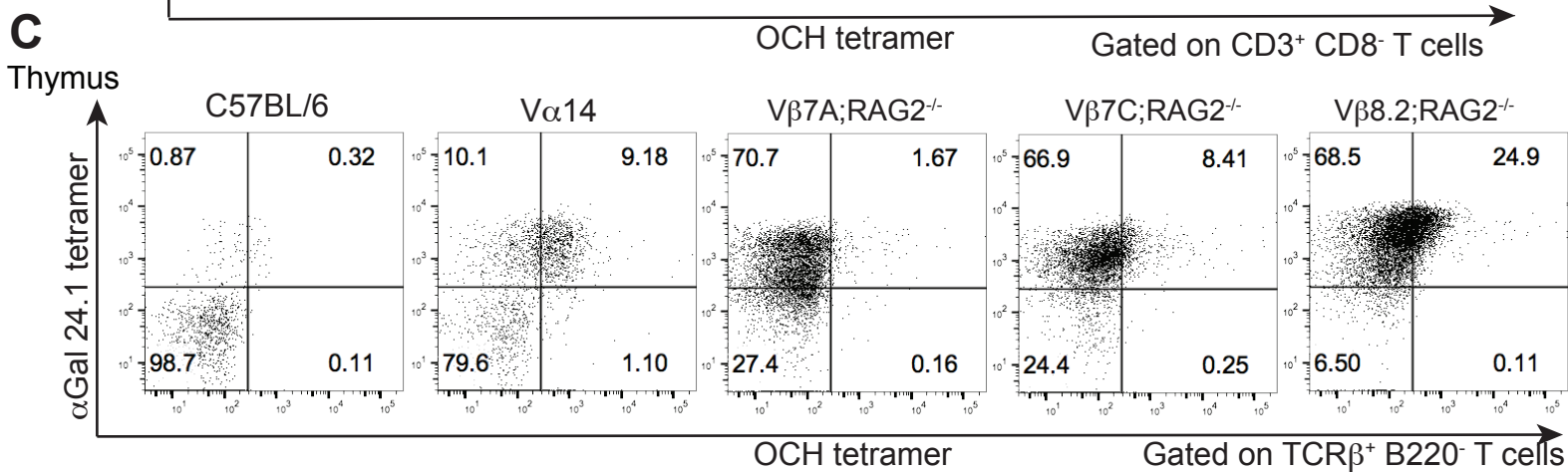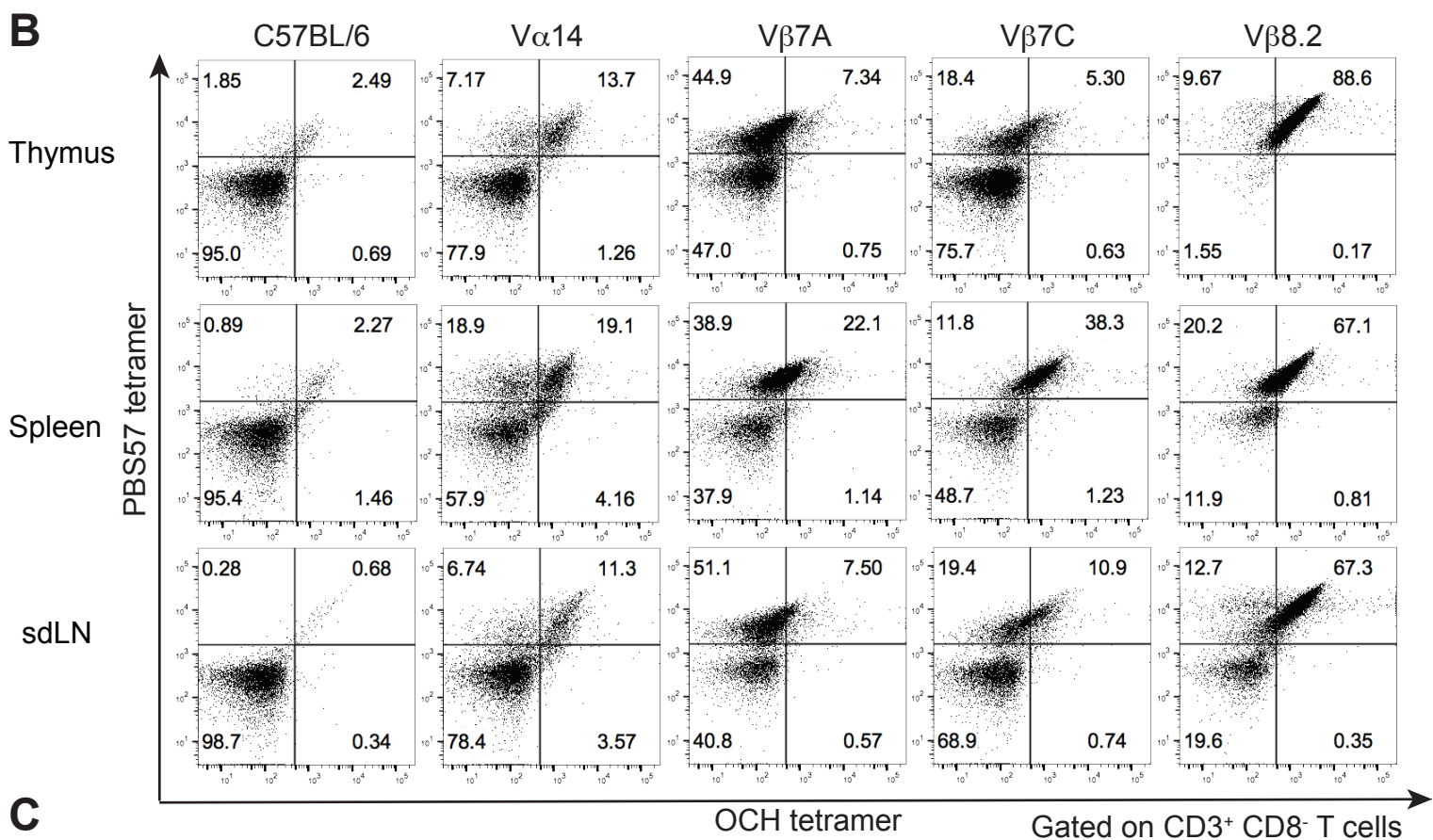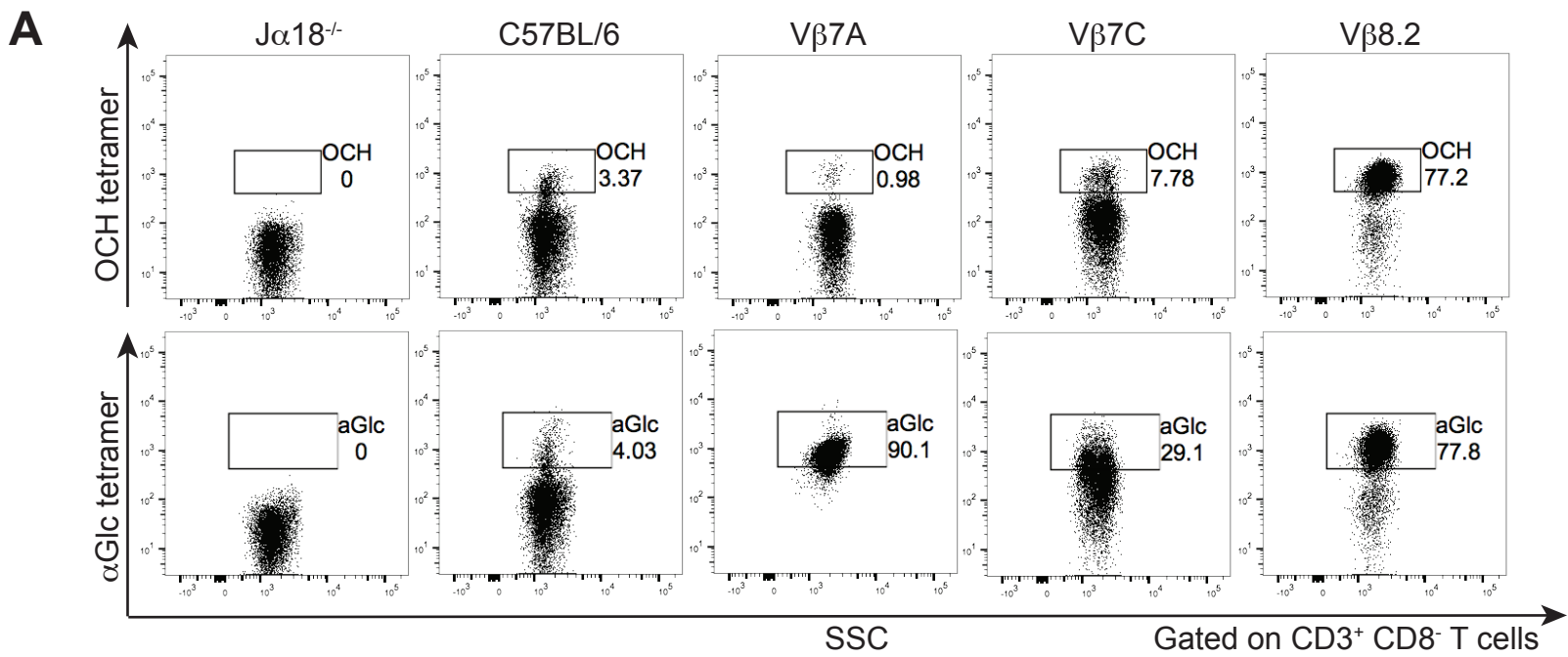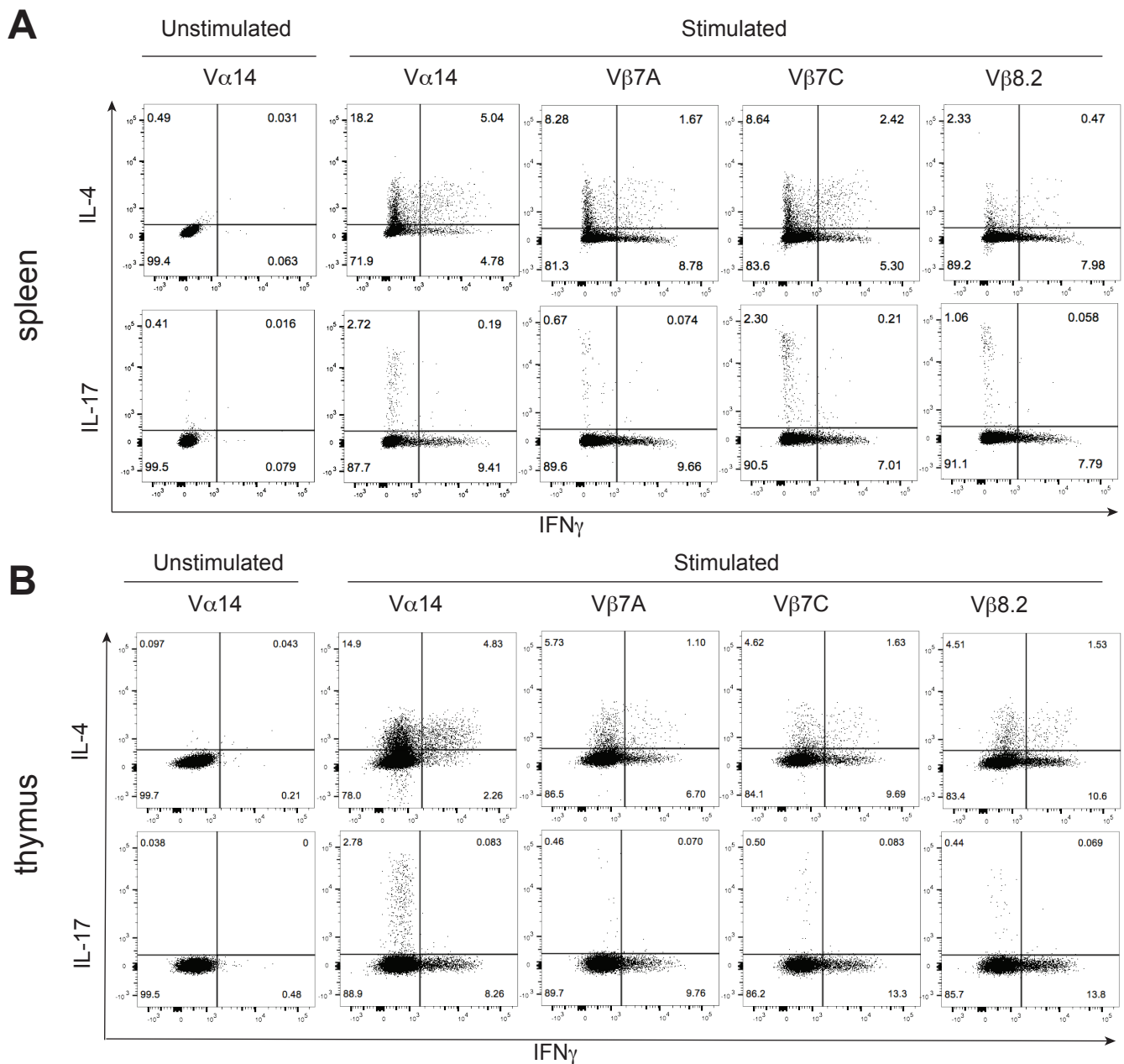
Supplemental Figure 1. Monoclonal iNKT cell mice have differing antigen preference. (A) Splenocytes from Jα18^{-/-}, C57BL/6, and indicated TN lines were harvested and stained with anti-CD3, anti-CD8, and either OCH tetramer or α-GlcCer tetramer, as indicated. **(B)** Thymus, spleen, and sdLN were harvested from C57BL/6 and indicated TN lines and stained with anti-CD3, anti-CD8, OCH, and PBS57 tetramers simultaneously. **(C)** Thymii from C57BL/6, Vα14, and monoclonal TN lines crossed onto a RAG2^{-/-} background were harvested and stained with TCRβ, B220, OCH tetramer, and α-GalCer (24.1) simultaneously. 24.1 represents a naturally occurring lipid tail length.
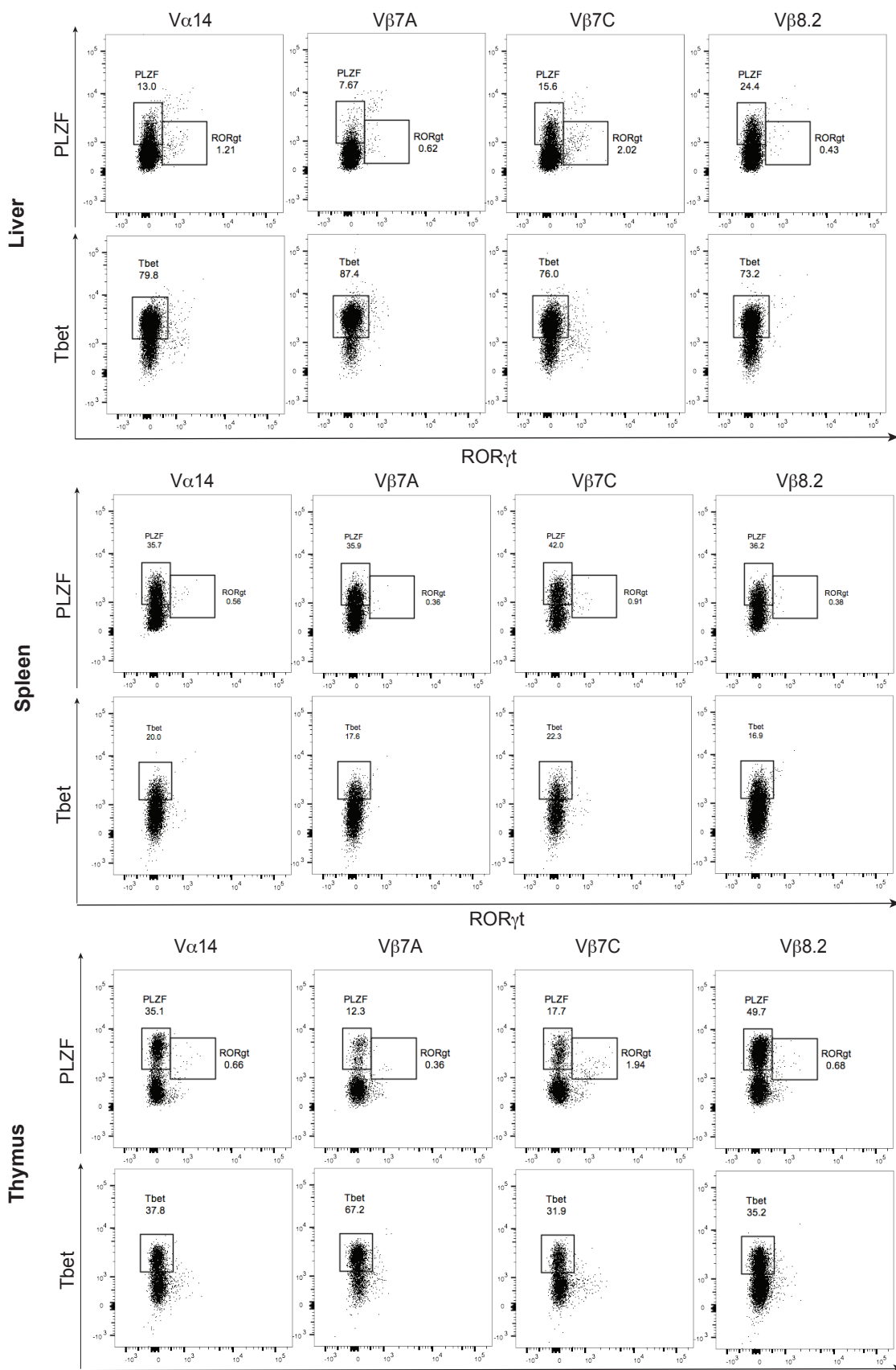
Supplemental Figure 1
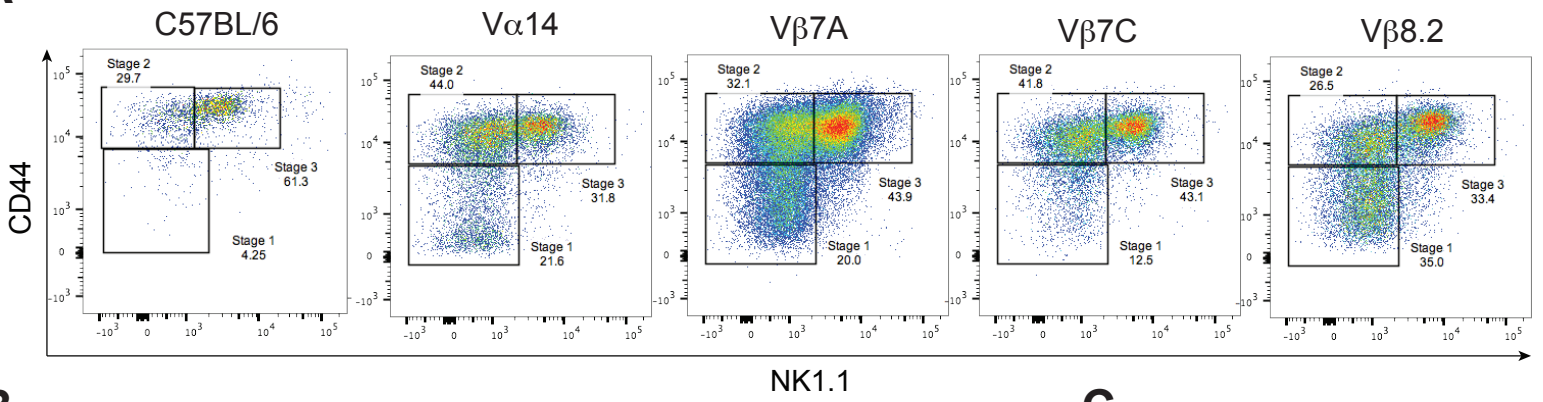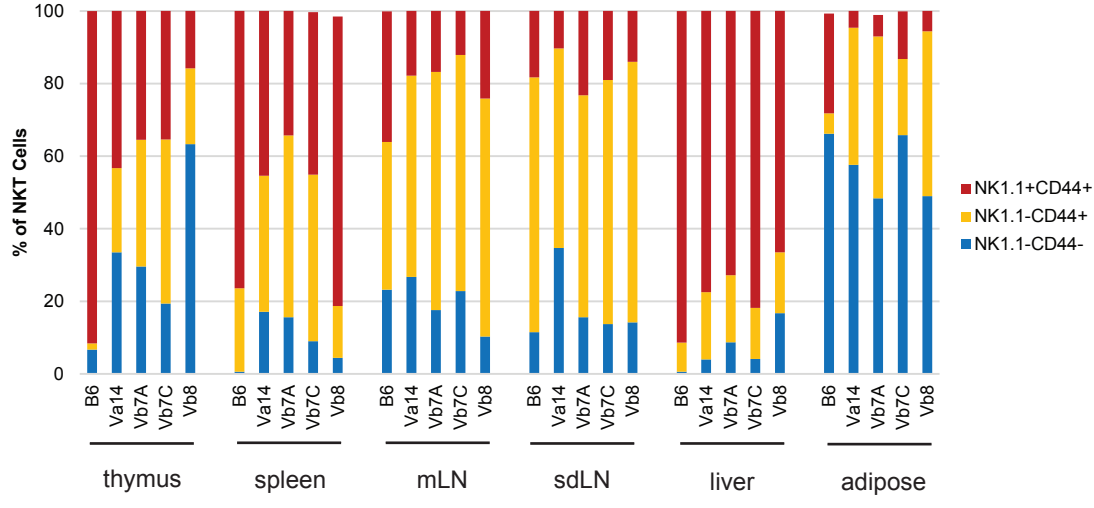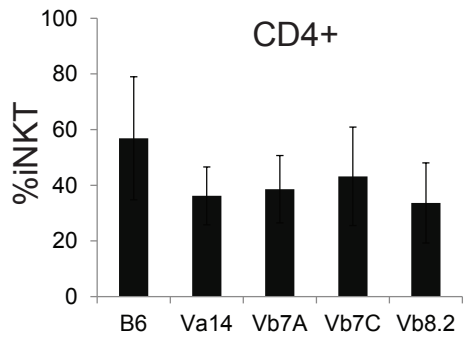
Supplemental Figure 2. CD44 and NK1.1 distribution is influenced by tissue of origin. (A) Thymocytes from each of the indicated mouse strains were stained with CD1d (PBS57) tetramer and antibodies to NK1.1, CD44, and CD4, and analyzed by flow cytometry. Representative flow plots are shown. n=3 mice per group. (B) iNKT cells from the indicated tissues analyzed as in (A) were quantified. Graph shows the percent iNKT cells in each gate, averaged from 3 mice per group. (C) Pooled spleen and lymph nodes from the indicated mouse strains were stained with CD1d (PBS57) tetramer and antibodies to CD3 and CD4, and analyzed by flow cytometry. Shown is the percent of iNKT cells that are CD4^{+}, averaged over 5 mice per group. Error bars are SD.

Supplemental Figure 3. Monoclonal iNKT cells on C57BL/6 background can produce all major cytokines. Cells from (A) spleen or (B) thymus of all TN lines were stimulated *in vitro* with PMA/Ionomycin for 4 hours, in the presence of GolgiStop. Cells were stained with anti-CD3 and CD1d (PBS57) tetramer, before being fixed, permeabilized, and stained with antibodies to IFNγ, IL-4, and IL-17. Results shown are gated on CD3$^+$CD1d-tetramer$^+$ cells.

Supplemental Figure 4. Distribution of iNKT cell subsets in liver of limited dilution bone marrow chimeras (BMC). Jα18$^{-/-}$ mice were lethally irradiated, reconstituted with 95% Jα18$^{-/-}$ bone marrow and 5% bone marrow of the indicated TN lines, and analyzed 8 weeks later. n=4 mice per group. Liver, spleen, and thymus cells from all BMC mice were stained with anti-CD3 and CD1d (PBS57) tetramer, before being fixed, permeabilized, and stained with antibodies to PLZF, Tbet, and RORγt. Results shown are gated on CD3^{+}CD1d-tetramer^{+} cells.

Supplemental Figure 4